Extended Reality for Preoperative Planning of Autologous Breast Reconstructions

T.M. (Tessa) Kos

Extended Reality for Preoperative Planning of Autologous Breast Reconstructions

By

Tessa Marianna Kos

to obtain the degree of

Master of Science
in Technical Medicine

at the Delft University of Technology,
to be defended publicly on Friday January 21, 2022 at 09:30 AM.

Student number: 4446844
Project duration: February 1, 2020 - January 21, 2022

Thesis committee:		
	Prof. dr. ir. J. Harlaar	TU Delft, 3mE
	Dr. E.M.L. Corten	Erasmus MC, Dept. Plastic, Reconstructive & Hand Surgery
	Dr. ir. T. van Walsum	Erasmus MC, Dept. Radiology & Nuclear Medicine, Biomedical Imaging Group Rotterdam

TU Delft

Preface

After six-and-a-bit years of education, of which the past year consisted of full-time research, this thesis marks the end of my time at Delft University of Technology, the Erasmus MC and the Leiden University Medical Center. I've started this project during my first internship at the Erasmus MC Department of Plastic, Reconstructive and Hand Surgery and I'm glad to have taken it to the next level by exploring future opportunities for preoperative planning in this field. This document contains the scientific article that describes our study design, methodology and results. The preceding literature review is of high relevance for our methods and can therefore be found in the appendix of this document.

The past months and this research have been an immense learning experience. Not only has this increased my knowledge on medical technology, its application and its use for improving diagnosis, treatment and care, but also about teamwork, communication and expectation management. It has made me realise that I really enjoy the puzzle that is scientific research and that I have a huge passion for this subject and its potential applications.

Although your thesis research is an individual project, I cannot say I have done it alone. I would like to thank my two direct supervisors Eveline and Theo for their enthusiasm, their help and their time. Thank you for listening to my ideas, your feedback and (occasionally) your voice of reason. Without you, I would not have enjoyed this project half as much. You have played a very important role over the course of the past 1,5 years and I would thoroughly like to thank you for it. In addition, I would also like to thank all my friends and family for their support. I could not have done it without them and I would definitely not have wanted to.

Tessa Marianna Kos

Delft, January 2022

Contents

1. Scientific Article 8
Extended Reality for Preoperative Planning of Autologous Breast Reconstructions: a Qualitative Study 9
Abstract 9
1. Introduction 9
2. Materials and Methods 11
2.1 Imaging Pipeline 11
2.2 Qualitative Pilot Study 12
3. Results 15
3.1 Imaging Pipeline 15
3.2 Qualitative Pilot Study 15
4. Discussion 19
4.1 Reflection 20
4.2 Future prospective 21
4.3 Limitations 22
5. Conclusion 22
2. References 23
3. Appendix 26
A. Literature review 26
Automated Detection of Small Vessels in Soft Tissues for Preoperative Planning – A Systematic Review 26
Abstract 26
Introduction 26
Methods 28
Results 29
Discussion 38
References 41
Appendix – Search Strings 48
B. Questionnaire 50
C. Questionnaire results 60
D. Additional comments questionnaire (literal transcription) 63

1. Scientific Article

Extended Reality for Preoperative Planning of Autologous Breast Reconstructions: a Qualitative Study

Abstract

Introduction The current gold standard for preoperative planning of deep inferior epigastric artery perforator (DIEAP) flap breast reconstruction is assessment of perforator vessels on computed tomography angiography (CTA) or magnetic resonance angiography (MRA) images in two-dimensional (2D) planes on a 2D screen. This research investigates the potential benefit of a 3D model of blood vessels on a 2D screen or Virtual Reality (VR) environment in preoperative planning for DIEAP flap breast reconstruction, compared to conventional CTA on a 2D screen.

Materials & Methods A qualitative study was conducted among six reconstructive plastic surgeons and four residents. Participants were asked to select the ideal perforator for unilateral DIEAP flap reconstruction in three viewing environments: conventional CTA in a 2D view, a 3D model in a 2D view and a 3D model in an immersive virtual reality (VR) view. Subsequently, a questionnaire on anatomical structure visibility assessing six perforator characteristics (perforator location in the flap, calibre, intramuscular course through the rectus abdominis, perforator origin, subcutaneous branching and connection to other vessels) was completed. Second, an adjusted Usefulness, Satisfaction and Ease of Use (USE) questionnaire on system usability was filled out.

Results Ten participants completed the experiments. The overall score distribution for perforator visibility characteristics was equal or higher except for perforator calibre in both 3D model views compared to conventional CTA. In the USE questionnaire, the 3D model in 2D view reported the highest scores for satisfaction and ease of learning. 90% of participants considered a 3D model in VR view to be of added value to preoperative planning, 60% considered a 3D model in 2D to be of added value. Overall, 40% would currently opt for the 3D model in a 2D view and 10% for the 3D model in a VR view.

Conclusion This study presents a perspective on the application of 3D models for preoperative planning in DIEAP flap breast reconstructions. There is an interest in use of a 3D model in a 2D view or an immersive VR environment to optimize preoperative planning. The visibility of important perforator characteristics received overall higher scores for the viewing environments with a 3D model, highlighting the potential benefit for 3D models and VR application for selection of ideal perforators in preoperative planning for DIEAP flap breast reconstructions.

Keywords *Breast Reconstruction, Deep Inferior Epigastric Artery Perforator Flap, Preoperative Planning, 3D model, Virtual Reality.*

1. Introduction

The deep inferior epigastric artery perforator (DIEAP) flap is the gold standard for autologous breast reconstructions following mastectomy. In DIEAP flap breast reconstructions, vascularized adipocutaneous tissue is transferred from the abdominal donor site to the chest. The DIEAP vessels and their corresponding veins are dissected through the rectus abdominis muscle, sparing as much of the muscular tissue as possible, and are reattached to the internal thoracic artery. The aesthetically satisfying achievable outcome and low donor site morbidity, when compared to non-autologous reconstructions and transverse rectus abdominis myocutaneous (TRAM) flaps respectively, makes the DIEAP flap reconstruction the preferred option (1, 2).

The DIEAP vessels emerge from the deep epigastric artery and are anatomically highly variable. Preoperative selection of the most suitable vessel for DIEAP flap reconstruction is an important component in the operative process and has shown to reduce operative time, surgeon stress and postoperative complications. Preoperative visualization of the deep abdominal vasculature using computed tomography angiography (CTA) or magnetic resonance angiography (MRA) imaging has proven accurate for identifying the most suitable DIEAP vessel for reconstruction (3, 4).

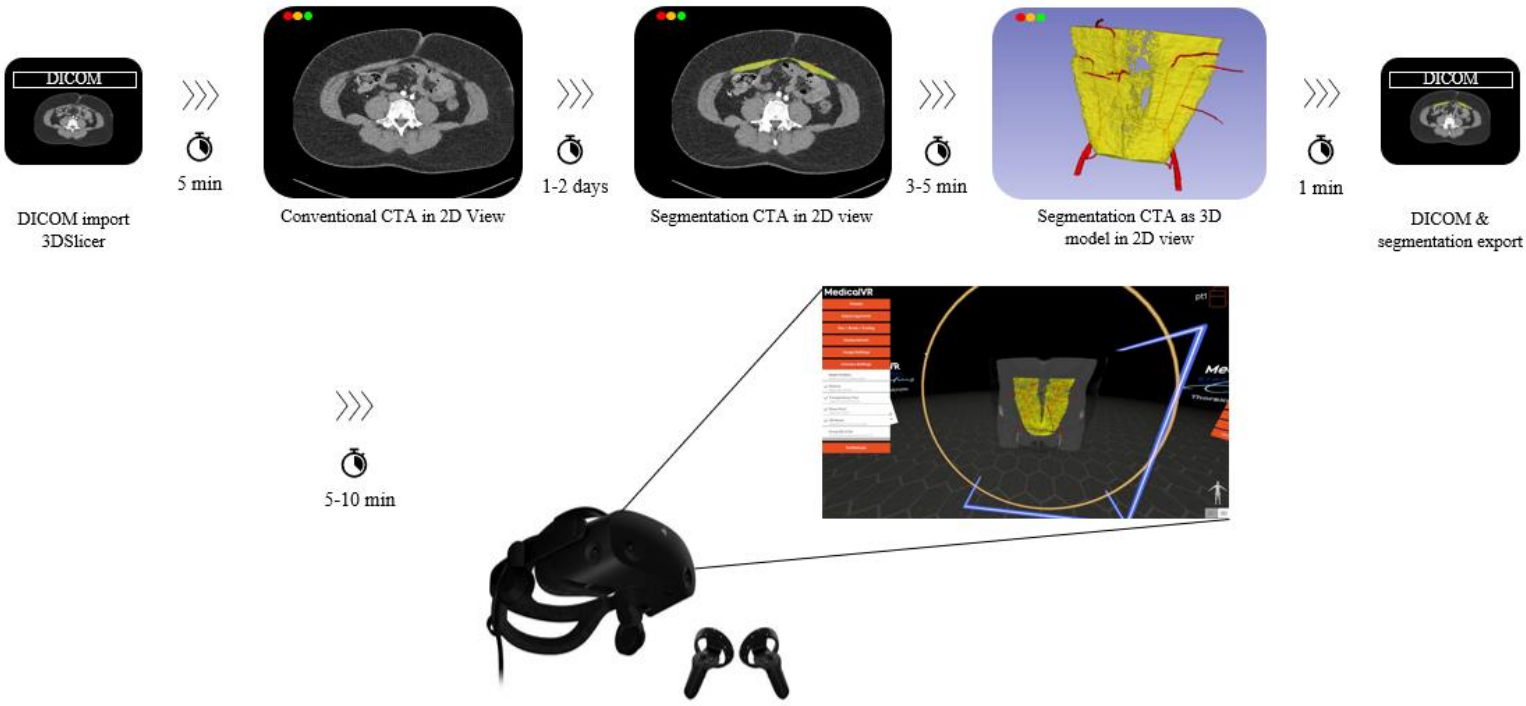

Figure 1. Image processing pipeline. DICOM files are imported into 3DSlicer. Conventional CTA is reviewed in 2D environment, then CTA is segmented semi-automatically. 3D segmentations are visualized as 3D models in 2D viewing environment, then the DICOM and segmentation (NIFTI) files are exported and uploaded to MedicalVR CT viewing environment software. The 3D model and CTA are visualized in an immersive VR environment using a head-mounted device.

The current gold standard visualization method for assessment of preoperative imaging for DIEAP flaps is two-dimensional (2D). Surgeons rely on memory and their ability to mentally reconstruct a three-dimensional (3D) map of the vascular structures that are presented in 2D, to translate their preoperative planning to the patient on the table. In the field of DIEAP flap reconstruction, 3D visualization and assessment of the vascular anatomy has been proposed in different visualization environments. Most solutions have described the projection of perforators on the abdomen prior to surgery or create a 3D-printed model of the abdominal vasculature (5-9). In other surgical specialties, 3D or extended reality (XR) visualization of anatomical structures is increasingly being used for preoperative planning and surgical training (10-14).

XR is an umbrella term for virtual reality (VR), augmented reality (AR) and mixed reality (MR). AR provides a user with a digital overlay to enhance the physical environment, e.g. by projecting a 3D object onto the patient or operating table. In a VR environment, users are fully immersed in a simulated world. VR creates an immersive environment by using displays that provide each eye with a separate image. A VR system uses cameras to match the physical movement in a digital world. MR is considered a blend of AR and VR, where the user can interact with digital objects in their physical environment (15). An immersive VR environment has shown to improve recall accuracy and spatial understanding when compared to 2D desktop displays, by involving vestibular and proprioceptive senses (16). Translating this to medical practice, an immersive VR environment could be valuable for improving the understanding of complex anatomical structures.

Although immersive VR environments have been used in surgical planning for several specialisms, this does not imply that it is directly applicable to preoperative planning of all surgical procedures (17). The complexity of visualizing the DIEAP vessels lies in their small size (diameter ~1.00-3.5mm) and their relatively low contrast-to-noise ratio (CNR) compared to their surrounding soft tissues (18). This complicates (automated) detection of these structures on routine CTA or MRA preoperative imaging. A preceding systematic review (Appendix A) has shown there is no automatic method for delineation of DIEAP vessels available yet. To the best of our knowledge, in DIEAP flap reconstruction

surgery, the utility of either a 3D visualization on a 2D screen or in an immersive VR environment for preoperative planning has not yet been studied compared to conventional CTA planning on a 2D screen. Therefore, in this paper we investigated the potential benefit of 3D visualization of perforator blood vessels in the abdominal wall in preoperative planning for DIEAP flap autologous breast reconstruction surgery compared to conventional CTA on a 2D screen and the contribution of the appearance of the 3D model, the viewing environment and the surgeon experience to this.

2. Materials and Methods

2.1 Imaging Pipeline

2.1.1 Image Acquisition

In the experiments, three abdominal CTA scans were used. These CTA scans were routinely acquired for preoperative planning of both unilateral and bilateral DIEAP flap reconstructions. The CTA scans were anonymized, and approval was obtained from the medical ethical review committee for use of the scans in studies investigating of DIEAP vessel segmentation and visualization for preoperative imaging. Two scans were photon-counting CTAs (PCCTA), acquired on a SIEMENS NAEOTOM Alpha, at 120 kVp tube voltage, 255 mA tube current, 0.4 mm single collimation width and 0.8 pitch factor. The scans were reconstructed with a slice thickness of 0.6 mm. One scan was a dual energy CTA (DECTA) made on a SIEMENS SOMATOM Force, at 80 kVp tube current, 98 mA tube current, 0.6 mm single collimation width and 0.6 pitch factor. This scan was reconstructed with a slice thickness of 1 mm.

2.1.2 Image Processing

A 3D model can be created by segmenting the structures of interest from an image by delineation, manually or (semi-) automatically. The complexity of the anatomical structures and several image qualities, amongst which spatial resolution of the imaging modality, the CNR and the overall signal-to-noise ratio (SNR) of the image could influence the segmentation quality and difficulty. For this study, 3D models of the rectus abdominis (RA) muscle and the DIEAP vessels were created from the PCCTA scans using the Segmentation Module in the 3DSlicer software[1], version 4.11.20210226 (19). For this, the Digital Imaging and Communications in Medicine (DICOM) files of the PCCTAs were loaded into 3DSlicer. The segmentation of the DIEAP vessels and RA muscle was performed semi-automatically, where the initial segmentations were generated using thresholding.

The threshold value was based on a trade-off between correctly segmenting muscle/vessel and including little noise in the segmentation. After thresholding, the segmentations were manually adjusted. In the segmentations of the RA muscle, noise was removed and holes were filled per slice. The segmentations of the DIEAP vessels were first adjusted per slice and subsequently in the 3D view. The subcutaneous branching was not included in the initial segmentations due to low contrast with the adipose tissue. Therefore, subcutaneous branching was manually segmented. After segmentation, 3D models were created based on the segmentations. For VR visualization, the models were exported as NIFTI (Neuroimaging Informatics Technology Initiative (nii.gz)) files. The full image processing workflow can be found in Figure 1.

2.1.3 Viewing Environment

Three different viewing environments of the abdominal CTAs were used: a viewing environment with the axial, sagittal and coronal slices of a conventional (non-segmented) abdominal CTA on a 2D screen, a 3D model of the RA muscle and the DIEAP vessels on a 2D screen and a 3D model of these structures in an immersive VR environment.

For visualization of the conventional CTA on a 2D screen and the 3D model on a 2D screen during the experiment, the 3DSlicer viewing environment was used (Figure 2, 3). Interaction with the conventional CTA was possible by scrolling through the slices and adjusting the region of interest using a mouse. For the 3D model in a 2D viewing environment, interaction with the model was also done through a mouse, allowing scaling and rotation of the model in all directions. It was possible to add the axial, sagittal and coronal CTA view, as well as a clipping plane (Figure 3). The VR model was visualized using the CT VR viewing software from MedicalVR[2], in combination

[1] https://www.slicer.org/

[2] https://www.medicalvr.eu/nl/

with a HP Reverb G2 VR headset. The HP Reverb G2 has a field of view of 110.9º, with a mura-free LCD panel of 2160x2160 pixels per eye. Interaction with the VR model was done through hand controllers, allowing rotation, scaling and use of a clipping plane in all directions.

2.2 Qualitative Pilot Study

2.2.1 Study Procedure

The participants were medical staff members and plastic surgery residents from the Department of Plastic, Reconstructive and Hand Surgery at the Erasmus MC in Rotterdam who perform DIEAP flap breast reconstructions on a regular basis. Participants with >15 years experience in DIEAP flap harvesting were asked to function as 'expert group'. Prior to the experiments, participants were informed that the results would be used anonymously for research purposes. In the experiments, participants were asked to use the three different planning environments as they would to prepare for a unilateral DIEAP flap reconstruction.

To minimize learning bias, scans from three different patients were used, one scan per viewing environment. Participants were asked to select one 'most suitable' DIEAP vessel in each viewing environment. After choosing a perforator, participants filled out a questionnaire assessing the visibility of structures and the system usability (Appendix B). They were allowed to re-evaluate the planning environment during the questionnaire.

The total study procedure is displayed in Figure 5. Participants got a short explanation for each viewing environment and their interaction controllers. Subsequently, for each viewing environment they got 10 minutes time, during which they were allowed to interact with the model by rotating, zooming, cutting through the 3D visualization and changing body surface opacity in any way they saw fit. Afterwards, they were asked to select the DIEAP vessel they considered 'most suitable' by marking its point of entering and leaving the RA muscle. For the VR environment, they were only asked to mark the 'entrance point', due to time restrictions and learning curve.

Figure 2. Non-segmented conventional CTA in 2D viewing environment.

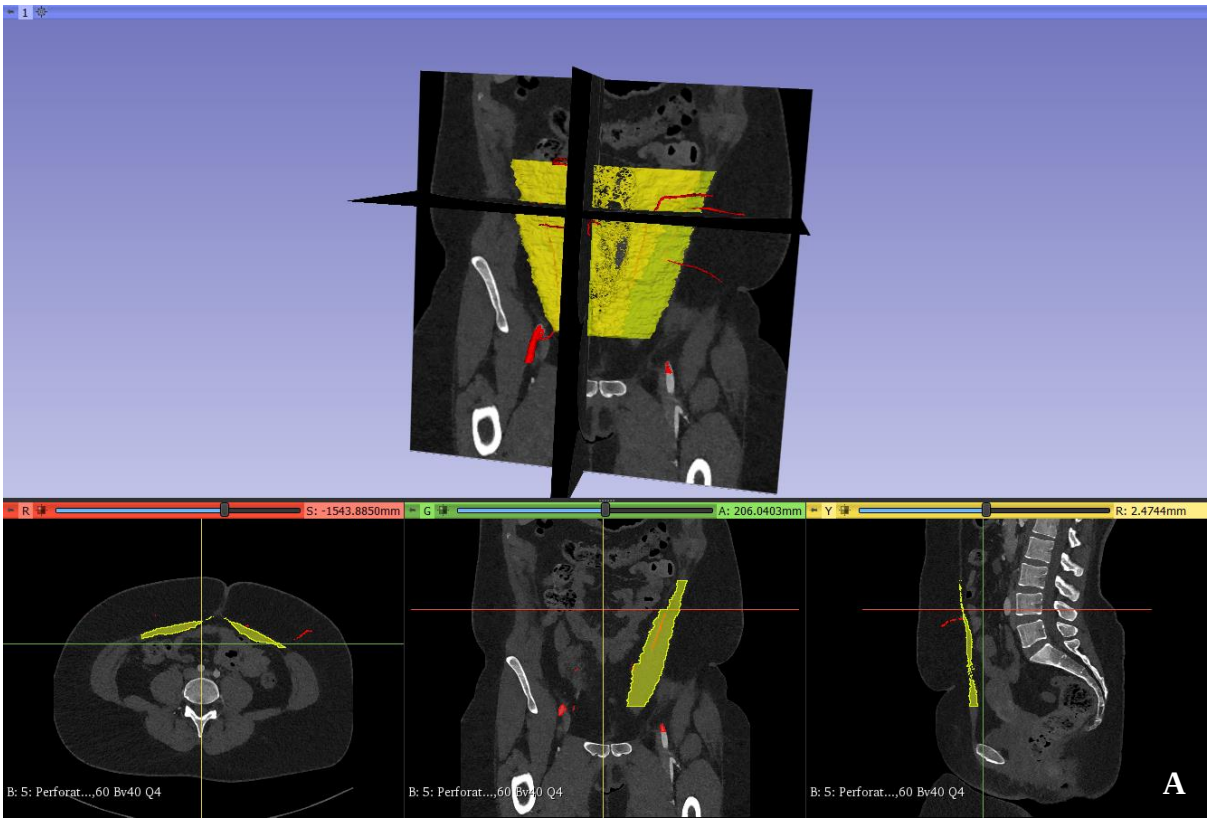

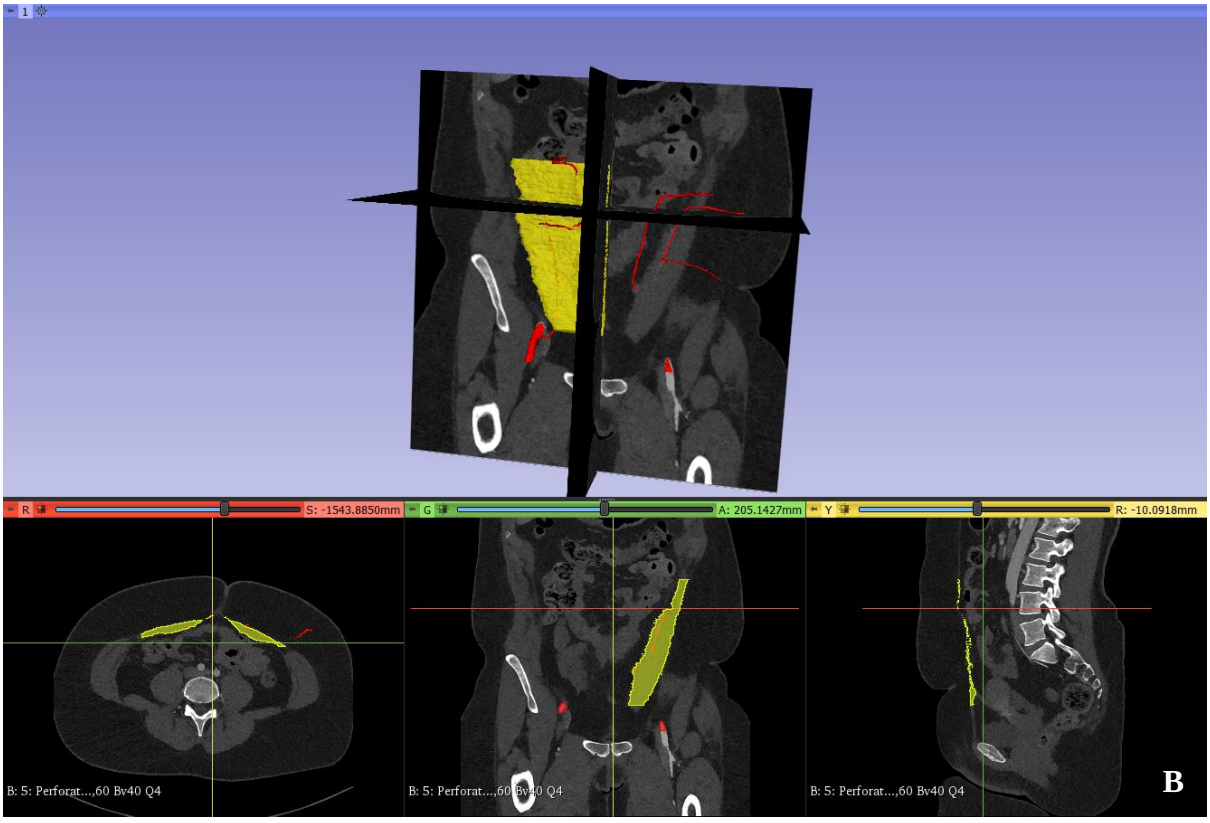

Figure 3. Segmented CTA and 3D model in 2D viewing environment without clipping plane (A) and with clipping plane (B).

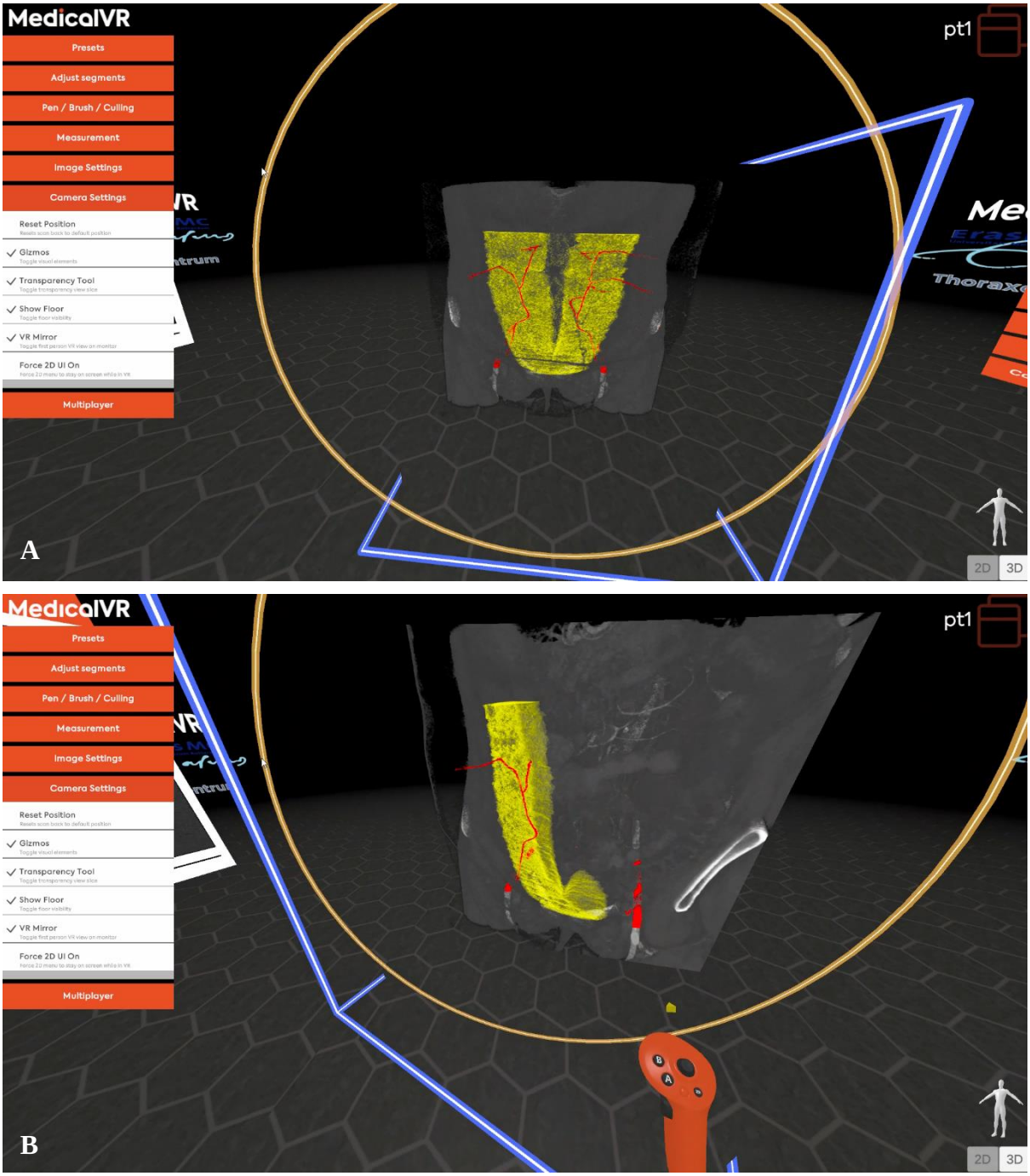

Figure 4. Segmented CTA and 3D model in immersive VR environment (MedicalVR), in frontal view (A) and with controller and clipping plane (B).

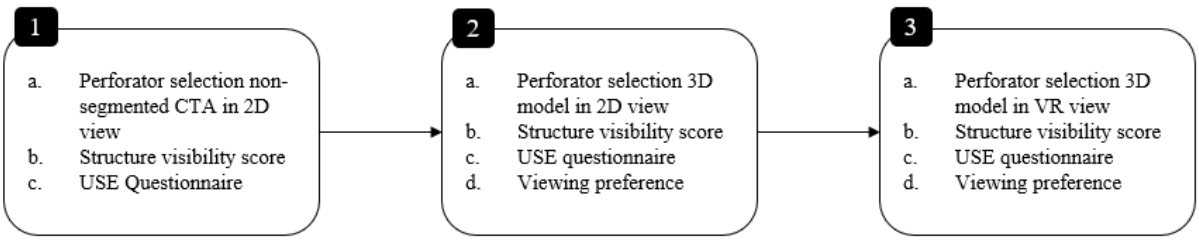

Figure 5. Study procedure qualitative pilot study

2.2.2 *Questionnaire*

Participants were asked to complete a questionnaire after each section of the experiment. The full questionnaire can be found in Appendix B. The questionnaire consisted of two or three components, depending on the section. The visibility of DIEAP vessels was assessed using six perforator characteristics which are considered important for preoperative mapping: perforator location in the flap, calibre, intramuscular course through the rectus abdominis, perforator origin, subcutaneous branching and connection to other vessels (2, 20-22). The second component was an adjusted USE questionnaire, assessing the usefulness, ease of use, ease of learning and satisfaction for each viewing environment (23). The adjusted USE questionnaire consisted of 16 questions. Structure visibility and the USE questionnaire were reported in a seven-point Likert scale, ranging from 'strongly disagree' to 'strongly agree'. For analysis, these rankings were assigned a numeric value between 1 and 7, where 1 corresponded to 'strongly disagree' and 7 to 'strongly agree'. Scores resulting from structure visibility and the USE questionnaire were calculated and visualized separately. The last component of the questionnaire inquired the attitude towards future use of 3D models in preoperative planning.

2.2.3 *Comment analysis*

Participants were asked to leave comments on the workflow, the model and additional remarks at the end of the questionnaire. These comments were categorized based on topic and reviewed as supplementary information.

Subject ID	Function	X years experience with DIEAP flap harvesting	Participation in X DIEAP flap reconstructions
1	Resident		>30
2	Staff member*	>15	
3	Staff member	5-10	
4	Resident		10-20
5	Staff member	10-15	
6	Staff member	0-5	20-30
7	Resident		>30
8	Staff member*	>15	
9	Staff member	0-5	20-30
10	Resident		10-20

Table 1. Participant demographics. * are selected as expert group. Staff members with 0-5 yeas experience with DIEAP flaps were also asked for their experience participating in DIEAP flaps.

3. Results

3.1 Imaging Pipeline

The full imaging pipeline is shown in Figure 1. In both 3D models, the DIEAP vessels were shown in red at 100% opacity and the rectus abdominis muscle was shown in yellow, at 25% opacity. The final 3D models can be found in Figure 6.

3.2 Qualitative Pilot Study

3.2.1 *Participant Demographics*

Ten volunteers took part in the experiments: six staff members and four plastic surgery residents. Table 1 shows the study population demographics. The 'expert group' consisted of two surgeons with >15 years experience with DIEAP flap harvesting and was used for gold standard comparison.

3.2.2 *Structure visibility*

Figure 7 shows the structure visibility scores. Box plots were used to visualize the data distribution into quartiles. The conventional CTA in 2D view was used as a reference environment. Calibre had a median and interquartile range (IQR) of 6(5.25;6), 5.5(3.25;6) and 5(3.5;5.75) for conventional CTA in 2D, 3D model in 2D view and 3D model in VR view respectively. Intramuscular course had a median and IQR of 6(3.5;6), 5.5(5;6) and 6(5;6.75) for conventional CTA in 2D, 3D model in 2D view and 3D model in VR view respectively. Location in flap had a median and IQR of 6(6;6), 5.5(4.25;6.75) and 6(5.25;6;75) for conventional CTA in 2D, 3D model in 2D view and 3D model in VR view respectively. Perforator origin had a median and IQR of 6(6;6), 6(5.25;6) and 5.5(5;6) for conventional CTA in 2D, 3D model in 2D view and 3D model in VR view respectively. Subcutaneous branching had a median and IQR of 3.5(3;5), 3.5(2;5.75) and 4.5(2;6) for conventional CTA in 2D, 3D model in 2D view and 3D model in VR view respectively. Lastly, connection to other vessels received a median and IQR of 3.5(2;4), 3.5(2;5) and 4.5(2.25;5.75) for conventional CTA in 2D, 3D

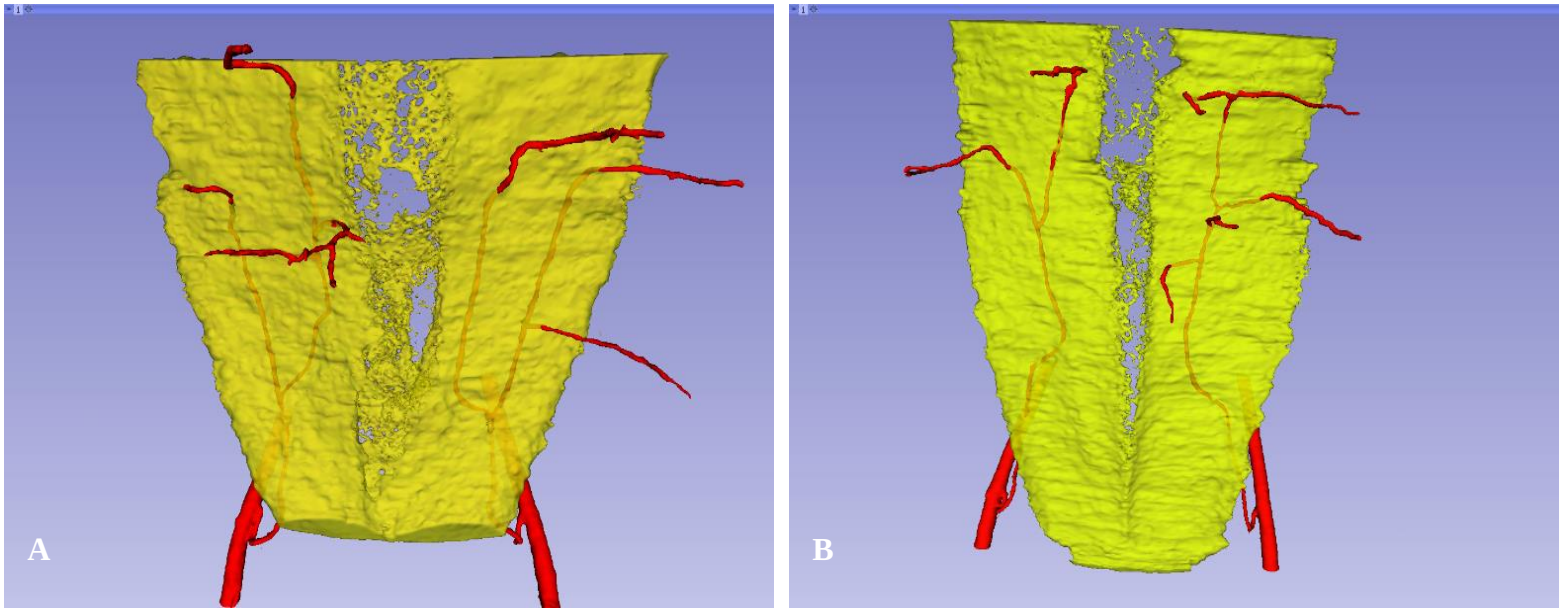

Figure 6. The two segmented 3D models: one for the 2D viewing environment (A) and one for the immersive VR environment (B).

model in 2D view and 3D model in VR view respectively.

Thus, for calibre visibility, the IQR is high for conventional CTA in 2D view, compared the other two viewing environments. For location in flap and perforator origin, the IQR is concentrated at 6, which is high compared to the 3D model in a 2D view. The 3D model in VR view has a less densely concentrated IQR than the conventional CTA, but is scored higher than the 3D model in 2D view for location in flap and perforator origin. For intramuscular course in 3D model in VR environment, the IQR is also higher than for the other two environments.

3.2.3 USE questionnaire

Figure 8 shows a visual representation of the average perceived USE values, per category for the different questions. The full results of the USE questionnaire can be found in Appendix C. Conventional CTA in 2D environment received a 5.5 average, compared to 4.4 and 4.6 for the 3D model in 2D view and VR view respectively. For ease of use, the CTA model received a 4.7, compared to a 4.5 and 4.6 for the 3D model in 2D view and VR view respectively. For satisfaction, conventional CTA and 3D in VR view received a 5.1 average, compared to a 4.5 for 3D in 2D view. For ease of learning, 3D in VR view received a 4.8, compared to a 4.6 and 4.4 for conventional CTA and 3D in 2D view respectively.

3.2.4 Attitude towards future use

Figure 9 shows the users opinion towards future use of the 3D models in preoperative planning. 80% of participants would prefer using a 3D model in a 2D viewing environment in addition to their current planning, but in only in combination with a visible CTA and cutting planes. 70% of participants would prefer a 3D model in an immersive VR environment in addition to conventional planning and 20% would even prefer it instead of additional planning. 60% of participants thought that use of a 3D model in a 2D viewing environment would improve preoperative planning. 90% of participants believed that use of a 3D model in an immersive VR environment would improve the preoperative planning of

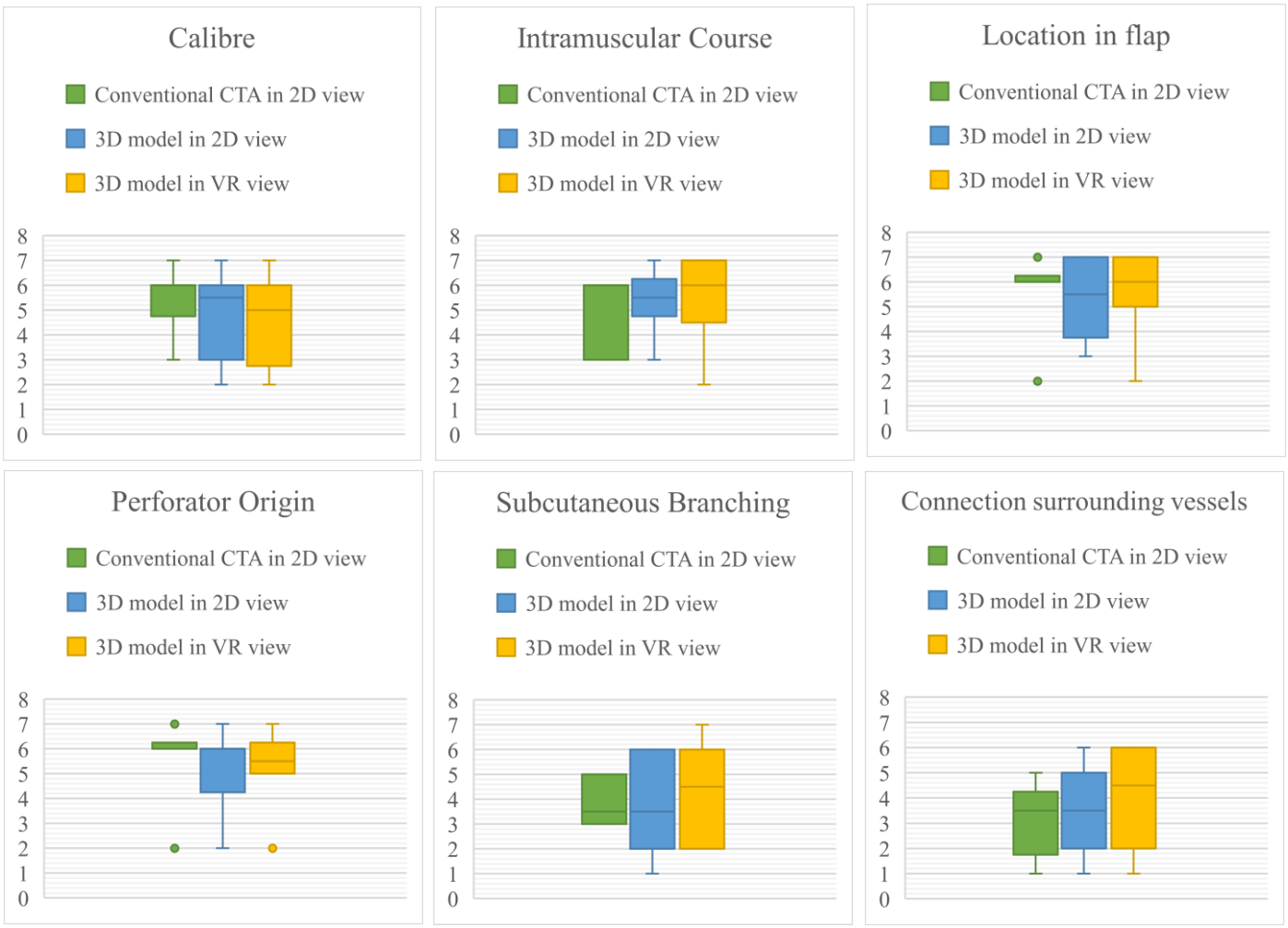

Figure 7. Box plots visualizing the data distributions of the structure visibility scores by a five-number summary for the six perforator characteristics: the division of data into quartiles. The y-axis shows the Likert scale scores (1-7). The minimum and maximum (non-outlier) values are visualized by the top and bottom lines. The box shows the first and third quartile and the line in the box is the median value. The small dots in 'Location in flap' and 'Perforator origin' are the outliers in the data, meaning they are a singular high or low value in the data distribution.

DIEAP flap reconstructions. One staff member believed that the 3D model in 2D or VR view would not be of additional value but would prefer the VR environment as addition to conventional planning.

Overall, 50% of participants would prefer to use conventional planning, 40% would prefer a 3D model in a 2D view and 10% would prefer to use the 3D model in an immersive VR

environment for preoperative planning. No structural difference between staff members and the plastic surgery residents was identified with regard to viewing preference.

3.2.5 Perforator choice

For each viewing environment, participants marked their most suitable perforator for unilateral DIEAP flap reconstruction and elaborated on their considerations for choosing this perforator. The perforator choices are depicted in Table 2. Each perforator was assigned a number, as shown in

Subject ID	CTA	3D	VR
1	R_1.3	R_2.3	X
2	R_1.2	R_2.1	X
3*	R_1.2	R_2.1	L_1.3
4	R_1.2	R_2.2	X
5	R_1.2	R_2.2	X
6	R_1.3	R_2.3	L_1.1
7	R_1.3	R_2.3	R_1.2
8*	R_1.2	L_1.1	L_1.1
9	R_1.2	R_2.1	L_1.1
10	L_1.1	R_2.3	L_1.2

Table 2. Perforator choice by participants. * are surgeons in 'expert group'. Each perforating vessel was assigned a number (e.g. R_1.1 is first perforating vessel of first intramuscular branch on the right side).

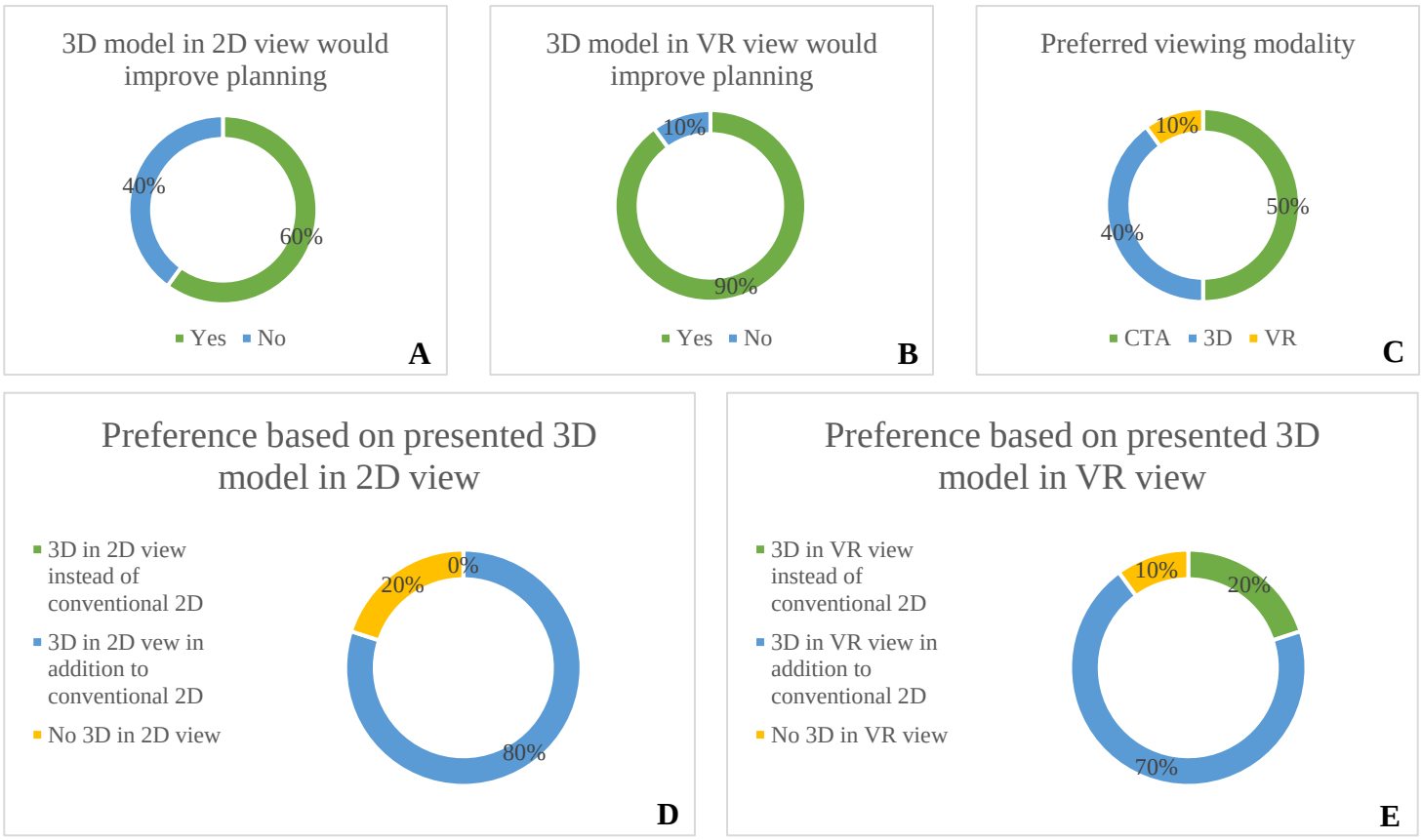

Figure 9. Pie charts visualizing the assessment of the benefit of a 3D model in 2D view (A) and a 3D model in VR view (B) for preoperative planning and the assessment of overall current preferred viewing modality (C). (D) and (E) visualize the preference for use of the 3D model in 2D view and in VR view regarding the currently presented model.

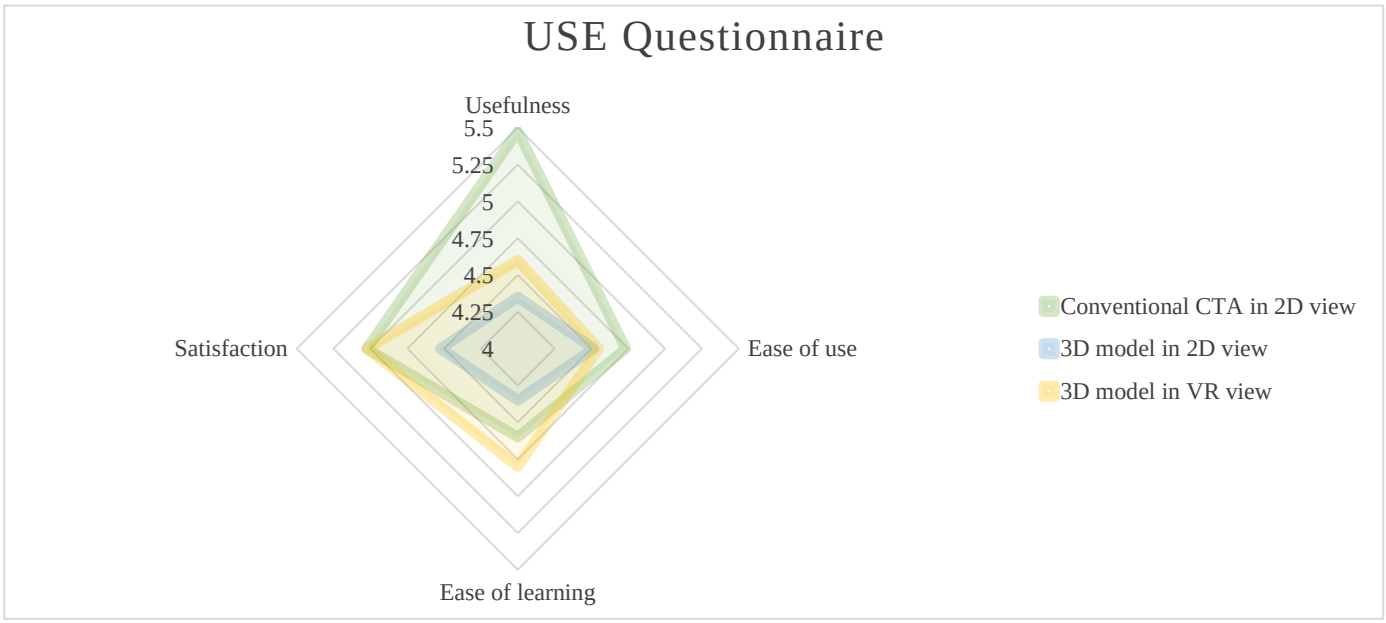

Figure 8. Radar chart visualizing the average results from the USE questionnaire in the categories Usefulness, Satisfaction, Ease of Use and Ease of Learning.

Figure 10 (e.g. R_1.1 was the first perforating vessel of the first intramuscular branch on the right side). Regarding the 2D visualization of the conventional planning, the expert group agreed on the most suitable perforator: R_1.2. 50% of participants agreed with this choice. Regarding the 3D model in a 2D view and in the immersive VR view, the expert group did not agree on the most suitable perforators.

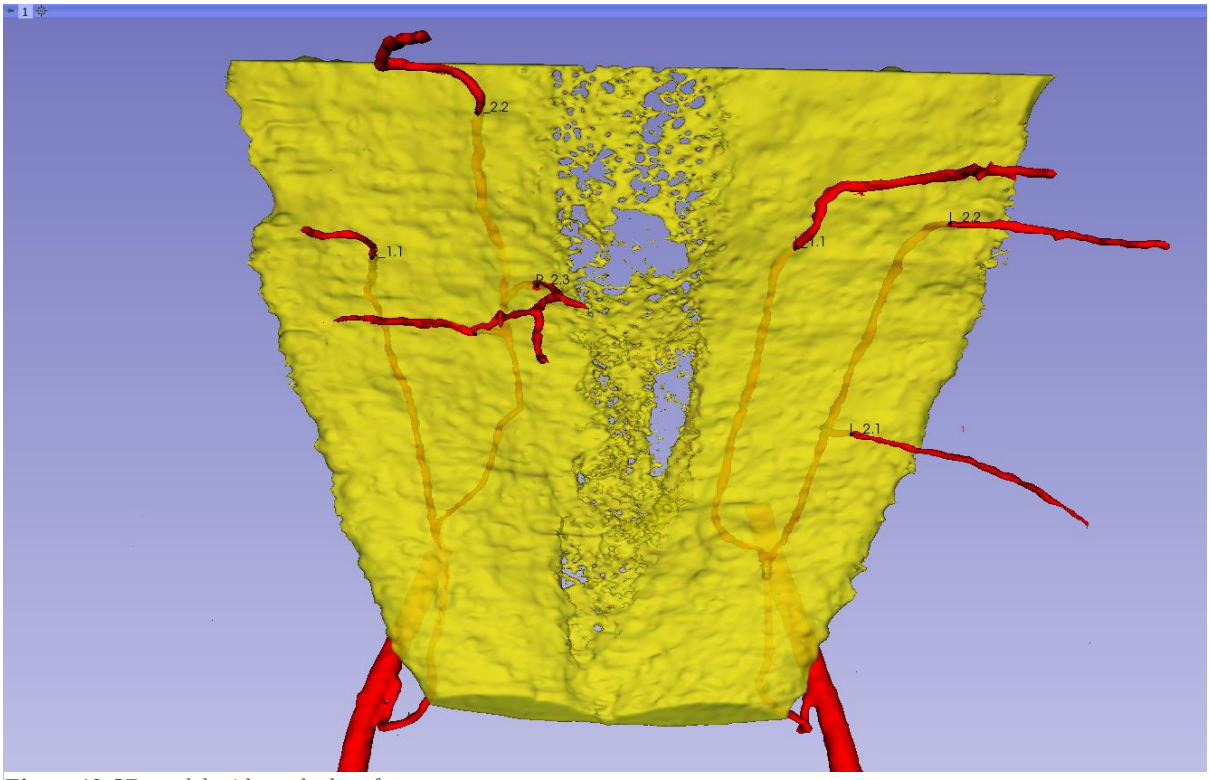

Figure 10. 3D model with marked perforators.

3.2.6 Comments

The exact comment transcription can be found in Appendix D. Table 3 shows the comment distribution into the categories. The comment topics could be divided into three categories: the segmentation of surgically relevant structures, the value of the 3D model and VR environment and the use and learning curve. The comments on segmentation cover the validity of the 3D model a participant is looking at. For the comments on the value of the 3D model/VR environment, the participant assumes the segmentation is close to reality but the functionality is not quite as they would wish. The comments on use of the viewing environments and learning curve provide insight the usability, assuming the segmentation is close to reality and the functionality would be as they wish.

Segmentation	Accuracy of segmentation compared to reality
	Calibre overestimation
	Match conventional CTA and real-life situation in patient
Value 3D model/VR environment	Improved vision on course
	Subcutaneous branching is not very clear in either of three visualizations
	VR environment looks great
	VR allows ‘airplane’ intramuscular view of vessels
Use and learning curve	Coordinates remain essential
	Selection on VR/3D but coordinates on CTA
	Steep learning curve especially on immersive VR environment

Table 3. Additional comments questionnaire.

4. Discussion

In this qualitative preclinical study we present our results and initial experience with the use of 3D models for preoperative planning of DIEAP flap breast reconstructions. The purpose of this study was to evaluate whether 3D models in a 2D or immersive VR viewing environment could be of additional value to a conventional CTA planning in a 2D viewing environment. Ultimately, providing a 3D visualization of the anatomical structures of interest prior to surgery could be of aid in translating the anatomical scans to the patient on the table and support the intraoperative decision-making process.

4.1 Reflection

4.1.1 Results

In our experiments, the visibility of perforator characteristics in the different viewing environments received similar scores. Calibre is scored higher in the conventional CTA in 2D view, possibly because of uncertainty in 3D model accuracy. For the perforator origin and location in flap, all environments scored high, but the data distribution was more densely concentrated for the conventional CTA. The intramuscular course overall scored the highest for the 3D model in VR view. For other structure visibilities, the score distribution for the differ notably.

Regarding the USE questionnaire, the conventional CTA mainly scored well in usefulness, possibly due to experience working with this viewing environment. The 3D model in VR view mainly scored well in satisfaction, possibly due to the sensation of being immersed in your preoperative planning. The 3D model in a 2D view received the lowest scores in all categories, which was striking because overall, the majority of participants believed that a 3D model in VR would be of added value to preoperative planning and half of the group would prefer a 3D model in addition to conventional planning. Furthermore, half of our study population would choose conventional planning as their planning environment of choice, based on the (expected) learning curve of the VR immersive viewing environment and the possible inaccuracies in the model presented due to manual blood vessel segmentation.

It is interesting that especially the 3D model in an immersive VR environment was scored well for all aspects, results show participants are of opinion that an immersive VR environment would improve planning and the majority of participants would like a 3D model in both 2D and VR in addition to conventional CTA in a 2D view, or even use VR instead of conventional CTA. However, in their final opinion on which planning type to use in which viewing environment, the majority of participants opts for conventional CTA in a 2D viewing environment.

This could be caused by a lack of confidence in use of the 3D models, due to a learning curve and uncertainties regarding the validity of the models, as participants mentioned in their additional comments.

4.1.2 Study Design

For these experiments, we provided participants with a 2D (conventional) visualization of an abdominal CTA, a 3D model of an abdominal CTA on a 2D screen and a 3D model of an abdominal CTA in an immersive VR environment. Each viewing environment contained one scan. Participants were asked to select the most suitable perforator, assess the structure visibility, usability, ease of use, ease of learning and satisfaction for each viewing environment. The main concerns raised by participants were related to the validity of image segmentation, the absence of possibilities for coordinate placement and the expected learning curve of 3D techniques. There was no validated automatic method available for the segmentation of the DIEAP vessels. Therefore, similar to other studies in the field of 3D visualization of DIEAP vessels, our segmentations were created semi-automatically, without external validation (5, 7, 24). As creating and validating an algorithm for segmentation of the DIEAP vessels would take both time and a large amount of annotated data, the focus of this study was on the possible benefit of the 3D model in different viewing environments and not on creating a robust and validated model.

The fact that several participants commented on the validity of the segmentations was interesting, mainly there were no comments on validity of conventional CTA images. In addition, the expert group did not agree on one most suitable perforator in both 3D model environments, but they did agree on the most suitable perforator in the conventional CTA in 2D view. This could be caused by the quality of the perforators in these patients or by a lack of experience with these techniques and a need for more patient-specific medical background information than just imaging to form a ‘gold standard’ perforator choice. For future research we would advise several additions to the current study protocol to be made, to increase study robustness and to allow these techniques to become clinically feasible.

4.2 Future prospective

4.2.1 Imaging

Current imaging is primarily focused on the deep arterial vascular system. The quality of imaging is of essential importance to the quality of a preoperative planning and a segmentation. There is no consensus in the literature on the use of CTA or MRA for preoperative planning of DIEAP flap reconstructions (25-27). To our knowledge, there are no studies using MRA for 3D preoperative visualization of the DIEAP flap anatomy. It would be interesting to assess whether this would improve segmentation of anatomical structures.

Additionally, it has been reported that venous congestion or insufficiency is one of the more common complications of DIEAP flap reconstructions (28). Literature suggests that preoperative identification of DIEAP vessels with an atypical or indirect venous connection to the superficial inferior epigastric vein reduces the risk of venous congestion in the DIEAP flap (29, 30). Similar to DIEAP selection, there is no consensus on the preferred imaging modality. Further research into combined arterial and venous preoperative imaging and the connections within the vascular system could improve DIEAP flap outcome.

4.2.2 Study Design

For a future study design, we would advise several adaptations to the current study protocol. In addition to the current non-segmented CTA in 2D view, the 3D model in 2D view and the 3D model in a VR environment, there could be a CTA in 2D view where structures of interest are delineated but no 3D model is visible. It would also be advised to use more than one scan per viewing environment.

Furthermore, ideally, for the introduction of segmented structures and 3D viewing environments into preoperative planning, segmentation of anatomical structures of interest should be performed automatically as manual segmentation of these structures is time-consuming and user-dependent. A validated automatic segmentation method increases robustness of the virtual representation of clinical structures as it removes observer variability. Other fields where 3D models and immersive VR environments have been introduced for surgical planning often deal with either large structures with a high contrast to their background or with availability of large annotated image databases (31-33). For the application of DIEAP flap planning, a preceding literature study has shown that no automated segmentation techniques are available yet. Therefore, an interesting option for future research is the development of a robust method for DIEAP vessel segmentation. This would have to be developed prior to clinical testing and application of the 3D models in clinical practice, as manual segmentation of these structures for every preoperative planning is not feasible. Creating such a model would necessitate a large, annotated database with abdominal CTAs or MRAs.

The measuring protocol itself could also be adapted. First, testing in a larger, multi-centre setting with more information on participants prior to experiments could be taken into consideration. Another study has researched the effect of 3D VR visualization of anatomical structures on the recall accuracy and confidence as a measure of added value over evaluation of structures in a 2D viewing environment, also taking into account the spatial abilities of participants (17). In the current study protocol, the natural learning curve including the ability for spatial understanding and stereopsis was not measured prior to the experiments. For further research into the application of a VR immersive environment for DIEAP flap preoperative planning, these aspects should be evaluated to eliminate confounding factors. A future study protocol would also include a more in-depth analysis of the use of viewing environment and comment analysis, by recording participants during experiments and/or structured interviews.

In these experiments, our expert group was considered the gold standard for perforator selection. However, they did not agree on the best perforator for all viewing environments, raising questions on the validity of a ‘gold standard’ based solely on imaging. A future study could also dive deeper into the whether all participants actually view the perforators similarly by asking them to trace the structures of interest rather than asking for the entrance and exit point of the perforator within the RA muscle.

4.3 Limitations

The study has a few limitations which should be taken into account when interpreting the data. First, the 3D models that were created for these experiments, were dependent on manual segmentation input. This may have resulted in a bias in assessing the 3D model viewing environments, especially regarding visibility of structures and perforator choice. Additionally, the study consisted of one measurement session per participant, for ten participants. One scan was used per viewing environment. These scans may not be representative for the average patient anatomy and due to the small study population, no statistical analysis was carried out.

Prior to these experiments, the users had no notable experience with a 3D model in the 2D or the VR environment, which might influence their opinion on these viewing environments and cause them to assign higher scores to a 'trusted' environment. Also, it was a single-centre study and all participants were employed at the Department of Plastic, Reconstructive and Hand Surgery in the Erasmus MC.

5. Conclusion

Overall, the findings from this study present a perspective on the application of 3D models for preoperative planning that, to our knowledge, has not been researched before. We have shown that there is an interest in use of a 3D model in a 2D view or an immersive VR environment in preoperative planning of DIEAP flap reconstructive surgery for surgeons in different levels of expertise. The visibility of important perforator characteristics received overall higher scores for the viewing environments with a 3D model, highlighting the possibility for 3D and VR application in this field. However, future experiments would have to prove the added value using a more robust segmentation method and a larger study population, also taking into considering the variety in natural visuospatial function and viewing environment functionalities.

2. References

1. Blondeel N, Vanderstraeten Gg Fau - Monstrey SJ, Monstrey Sj Fau - Van Landuyt K, Van Landuyt K Fau - Tonnard P, Tonnard P Fau - Lysens R, Lysens R Fau - Boeckx WD, et al. The donor site morbidity of free DIEP flaps and free TRAM flaps for breast reconstruction. (0007-1226 (Print)).
2. Healy C, Ramakrishnan V. Autologous Microvascular Breast Reconstruction. Arch Plast Surg. 2013;40(1):3-10.
3. Rozen W, Ashton M, Stella D, Phillips T, Grinsell D, Taylor G. The Accuracy of Computed Tomographic Angiography for Mapping the Perforators of the Deep Inferior Epigastric Artery: A Blinded, Prospective Cohort Study. Plastic and reconstructive surgery. 2008;122:1003-9.
4. Rodkin B, Hunter-Smith DJ, Rozen WM. A review of visualized preoperative imaging with a focus on surgical procedures of the breast. Gland Surgery; Vol 8, Supplement 4 (October 2019): Gland Surgery (Visualized Surgical Procedures of the Breast). 2019.
5. Wesselius TS, Meulstee JW, Luijten G, Xi T, Maal TJJ, Ulrich DJO. Holographic Augmented Reality for DIEP Flap Harvest. Plastic and Reconstructive Surgery. 2021;147(1).
6. Jablonka EM, Wu RT, Mittermiller PA, Gifford K, Momeni A. 3-DIEPrinting: 3D-printed Models to Assist the Intramuscular Dissection in Abdominally Based Microsurgical Breast Reconstruction. Plastic and Reconstructive Surgery – Global Open. 2019;7(4).
7. Chae MP, Hunter-Smith DJ, Chung RD, Smith JA, Rozen WM. 3D-printed, patient-specific DIEP flap templates for preoperative planning in breast reconstruction: a prospective case series. Gland Surgery; Vol 10, No 7 (July 2021): Gland Surgery. 2021.
8. Fitoussi A, Tacher V, Pigneur F, Heranney J, Sawan D, Dao TH, et al. Augmented reality-assisted deep inferior epigastric artery perforator flap harvesting. Journal of Plastic, Reconstructive & Aesthetic Surgery. 2021;74(8):1931-71.
9. Gacto-Sánchez P, Sicilia-Castro D, Gómez-Cía T, Lagares A, Collell T, Suárez C, et al. Use of a Three-Dimensional Virtual Reality Model for Preoperative Imaging in DIEP Flap Breast Reconstruction1. Journal of Surgical Research. 2010;162(1):140-7.
10. Gehrsitz P, Rompel O, Schöber M, Cesnjevar R, Purbojo A, Uder M, et al. Cinematic Rendering in Mixed-Reality Holograms: A New 3D Preoperative Planning Tool in Pediatric Heart Surgery. Frontiers in Cardiovascular Medicine. 2021;8:38.
11. Huettl F, Saalfeld P, Hansen C, Preim B, Poplawski A, Kneist W, et al. Virtual reality and 3D printing improve preoperative visualization of 3D liver reconstructions—results from a preclinical comparison of presentation modalities and user's preference. Annals of Translational Medicine; Vol 9, No 13 (July 2021): Annals of Translational Medicine. 2021.
12. Sadeghi A, Bakhuis W, van Schaagen F, Oei F, Bekkers J, Maat A, et al. Immersive 3D virtual reality imaging in planning minimally invasive and complex adult cardiac surgery. European Heart Journal - Digital Health. 2020;1:62-70.
13. Shirk JD, Thiel DD, Wallen EM, Linehan JM, White WM, Badani KK, et al. Effect of 3-Dimensional Virtual Reality Models for Surgical Planning of Robotic-Assisted Partial Nephrectomy on Surgical Outcomes: A Randomized Clinical Trial. JAMA Network Open. 2019;2(9):e1911598-e.
14. Robiony M, Salvo I, Costa F, Zerman N, Bazzocchi M, Toso F, et al. Virtual Reality Surgical Planning for Maxillofacial Distraction Osteogenesis:

The Role of Reverse Engineering Rapid Prototyping and Cooperative Work. Journal of Oral and Maxillofacial Surgery. 2007;65(6):1198-208.
15. Andrews C, Southworth MK, Silva JNA, Silva JR. Extended Reality in Medical Practice. (1092-8464 (Print)).
16. Krokos E, Plaisant C, Varshney A. Virtual memory palaces: immersion aids recall. Virtual Reality. 2019;23(1):1-15.
17. Hattab G, Hatzipanayioti A, Klimova A, Pfeiffer M, Klausing P, Breucha M, et al. Investigating the utility of VR for spatial understanding in surgical planning: evaluation of head-mounted to desktop display. Scientific Reports. 2021;11(1):13440.
18. Ayhan S, Oktar SO, Tuncer S, Yucel C, Kandal S, Demirtas Y. Correlation between vessel diameters of superficial and deep inferior epigastric systems: Doppler ultrasound assessment. J Plast Reconstr Aesthet Surg. 2009;62(9):1140-7.
19. Fedorov A, Beichel R Fau - Kalpathy-Cramer J, Kalpathy-Cramer J Fau - Finet J, Finet J Fau - Fillion-Robin J-C, Fillion-Robin Jc Fau - Pujol S, Pujol S Fau - Bauer C, et al. 3D Slicer as an image computing platform for the Quantitative Imaging Network. (1873-5894 (Electronic)).
20. Thimmappa N, Bhat AP, Bishop K, Nagpal P, Prince MR, Saboo SS. Preoperative cross-sectional mapping for deep inferior epigastric and profunda artery perforator flaps. (2223-3652 (Print)).
21. Uppal RS, Casaer B, Van Landuyt K, Blondeel P. The efficacy of preoperative mapping of perforators in reducing operative times and complications in perforator flap breast reconstruction. Journal of Plastic, Reconstructive & Aesthetic Surgery. 2009;62(7):859-64.
22. Wong KK, Stubbs E, McRae M, McRae M. CTA in preoperative planning for DIEP breast reconstruction: what the reconstructive surgeon wants to know. A modified Delphi study. Clinical Radiology. 2019;74(12):973.e15-.e26.
23. Lund A. Measuring Usability with the USE Questionnaire. Usability and User Experience Newsletter of the STC Usability SIG. 2001;8.
24. Hummelink S, Hameeteman M, Hoogeveen Y, Slump CH, Ulrich DJO, Schultze Kool LJ. Preliminary results using a newly developed projection method to visualize vascular anatomy prior to DIEP flap breast reconstruction. Journal of Plastic, Reconstructive & Aesthetic Surgery. 2015;68(3):390-4.
25. Cina A, Barone-Adesi L Fau - Rinaldi P, Rinaldi P Fau - Cipriani A, Cipriani A Fau - Salgarello M, Salgarello M Fau - Masetti R, Masetti R Fau - Bonomo L, et al. Planning deep inferior epigastric perforator flaps for breast reconstruction: a comparison between multidetector computed tomography and magnetic resonance angiography. (1432-1084 (Electronic)).
26. Vasile JV, Levine JL. Magnetic resonance angiography in perforator flap breast reconstruction. (2227-684X (Print)).
27. Mohan AT, Saint-Cyr M. Advances in imaging technologies for planning breast reconstruction. (2227-684X (Print)).
28. Gill PS, Hunt Jp Fau - Guerra AB, Guerra Ab Fau - Dellacroce FJ, Dellacroce Fj Fau - Sullivan SK, Sullivan Sk Fau - Boraski J, Boraski J Fau - Metzinger SE, et al. A 10-year retrospective review of 758 DIEP flaps for breast reconstruction. (0032-1052 (Print)).
29. Schaverien MV, Ludman Cn Fau - Neil-Dwyer J, Neil-Dwyer J Fau - Perks AGB, Perks Agb Fau - Raurell A, Raurell A Fau - Rasheed T, Rasheed T Fau - McCulley SJ, et al. Relationship between venous congestion and intraflap venous anatomy in DIEP flaps using contrast-enhanced magnetic resonance angiography. (1529-4242 (Electronic)).
30. Davis CA-O, Jones L, Tillett RL, Richards H, Wilson SM. Predicting venous congestion before DIEP breast

reconstruction by identifying atypical venous connections on preoperative CTA imaging. (1098-2752 (Electronic)).
31. Sadeghi A, Maat A, Taverne Y, Cornelissen R, Dingemans A-M, Bogers A, et al. Virtual Reality and Artificial Intelligence for 3D Planning of Lung Segmentectomies. JTCVS Techniques. 2021;7.
32. Fick T, van Doormaal JAM, Tosic L, van Zoest RJ, Meulstee JW, Hoving EW, et al. Fully automatic brain tumor segmentation for 3D evaluation in augmented reality. Neurosurgical Focus. 2021;51(2):E14.
33. Boedecker C, Huettl F, Saalfeld P, Paschold M, Kneist W, Baumgart J, et al. Using virtual 3D-models in surgical planning: workflow of an immersive virtual reality application in liver surgery. Langenbeck's Archives of Surgery. 2021;406(3):911-5.

3. Appendix

A. Literature review

Automated Detection of Small Vessels in Soft Tissues for Preoperative Planning – A Systematic Review

Abstract

Introduction The preoperative planning of deep inferior epigastric artery perforator (DIEAP) vessels is aimed at the tiny vessels of the donor site. Accurate segmentation of the DIEAP vessels is necessary for facilitating 3D visualization of the preoperative planning of DIEAP flap autologous breast reconstruction. This systematic review evaluates methods available for blood vessel segmentation (BVS), specifically for small vessels in soft tissues.

Methods A systematic search was conducted in Embase, Medline ALL (Ovid), Web of Science Core Collection, Cochrane and Google Scholar on March 23rd 2021. All literature on soft tissues imaged using computed tomography angiography (CTA) or magnetic resonance angiography (MRA), vessel segmentation as primary study subject and a clinical application for the segmentation method were included.

Results 66 articles were considered eligible for review. 29 articles presented a method for segmentation of an anatomical region where the smallest vessels would be classified as supermicrovessels. One article presented a method where the full vessel range was classified as supermicrovessels. Six articles presented a method for segmentation of an anatomical region where the smallest vessels would be classified as microvessels and one article presented a method where the full vessel range was classified as microvessels(1). The majority of methods was fully automatic, 12 articles required user input for their BVS method.

Conclusion Several methods show promising results in automated small vessel segmentation but they are a long way from the clinical practice. Further research testing the performance of promising fully automated methods on small vessels with low contrast, investigating the importance of vessel segmentation for 3D visualization of preoperative planning and evaluating the clinical benefit of improving preoperative planning for DIEAP flap autologous breast reconstructions is necessary.

Keywords Vascular Segmentation, Segmentation Algorithm, Preoperative Planning, Deep Inferior Epigastric Artery Perforator, Autologous Breast Reconstruction.

Introduction

Medical imaging technology plays an increasingly important role in planning plastic surgical procedures. The main purpose of preoperative planning in plastic surgery is identification of surgical target structures, access points and surgical paths, to cause minimal damage to surrounding tissues (2). For autologous breast reconstructions in breast cancer patients, a perforator flap is the treatment of choice (as opposed to a musculocutaneous flap) to minimize donor site morbidity without compromising aesthetic outcomes or patient safety. A perforator flap reconstruction uses abdominal adipocutaneous tissue and relies on the deep inferior epigastric artery perforator (DIEAP) vessels for perfusion of skin and tissue (3). A computed tomography angiography (CTA) image or a magnetic resonance angiography (MRA) image of the donor site and DIEAP vessels is made prior to the reconstruction. Preoperative mapping of the DIEAP vessels and their path through the rectus abdominis muscle on these images has been shown to reduce complications and operative time (4). The technical basis of image-based preoperative perforator mapping consists of multiple steps. Radiological imaging, pre-treatment image processing including region

of interest (ROI) selection and volumetric visualizations, the segmentation of structures of interest and (interactive) visual exploration of the DIEAP vessels (2).

In other surgical fields, such as liver, cardiothoracic and head and neck surgery, three-dimensional (3D) exploration of relevant structures has been suggested to improve quality of preoperative planning compared to 2D viewing of the radiological images. This can be done through a 3D rendering in the radiological viewer or through extended (or immersive) reality (XR) applications, which include augmented reality (AR), mixed reality (MR) and virtual reality (VR) environments (5-8). In this paper, VR refers to a full simulated environment where users interact with that environment other than the one they are actually in. AR refers to a virtual layer superimposed on a user's physical environment, which can add textual information or other virtual items. In MR, both virtual and physical objects are present and interaction with virtual objects is possible (9).

However promising, these techniques generally focus on surgeries of large vessels or bony structures. They are relatively easy to segment from a medical image without user input due to their size and visible intensity differences. Vessels for microsurgery (diameter ~1 mm) (10), for supermicrosurgery (diameter <0.8 mm) (11) or structures with low contrast compared to their surroundings are hard to distinguish on CTA or MRA imaging and thus hard to segment.

Despite its complexity, blood vessel segmentation (BVS) is a popular research field. In previous works, various groups have reviewed BVS techniques (12-15). They covered methods and evaluation metrics for different anatomical regions and imaging modalities. Kirbas and Quek (12) provide a global overview of BVS techniques, namely the pattern recognition techniques, model-based approaches, tracking-based approaches and artificial intelligence (AI)-based approaches. Lesage et al. (13) review general lumen segmentation techniques, focused on 3D imaging modalities. They discuss why proposed combinations of techniques are relevant in the field of BVS. Moccia et al. (14) provide a more recent analysis of BVS methods, looking at machine learning (ML) approaches, deformable models, tracking methods, performance evaluation metrics and databases used for the development of the BVS methods. Most recently, Zhao et al. (15) published a review on rule-based and machine-learning BVS methods. The prevalent conclusion from these reviews is that there is no single segmentation approach that can be used for all applications, mainly due to variance in appearance of anatomical regions on different imaging modalities. Additionally, a lack of systematic evaluation workflow due to little shared data and algorithms makes inter-algorithm comparison difficult. Thus, algorithm quality is difficult to compare objectively. Another prevalent conclusion is the necessity of hybrid methods, combining different techniques, and the increasing popularity of ML (specifically deep learning (DL)) for BVS. However, the most recent review was published in 2017, thus not taking into account the most recent progress in the field. In addition, these reviews cover BVS in the general sense and are not specific to (super)microvessels and/or low contrast differentiation.

In this paper, we focus on recent advancements in BVS. For our application, the topic of vessel segmentation for (super)microsurgery in MRA and CTA imaging and the potential translation to a 3D (XR) environment are the most relevant. The objective of this systematic review is to evaluate and compare methods available for

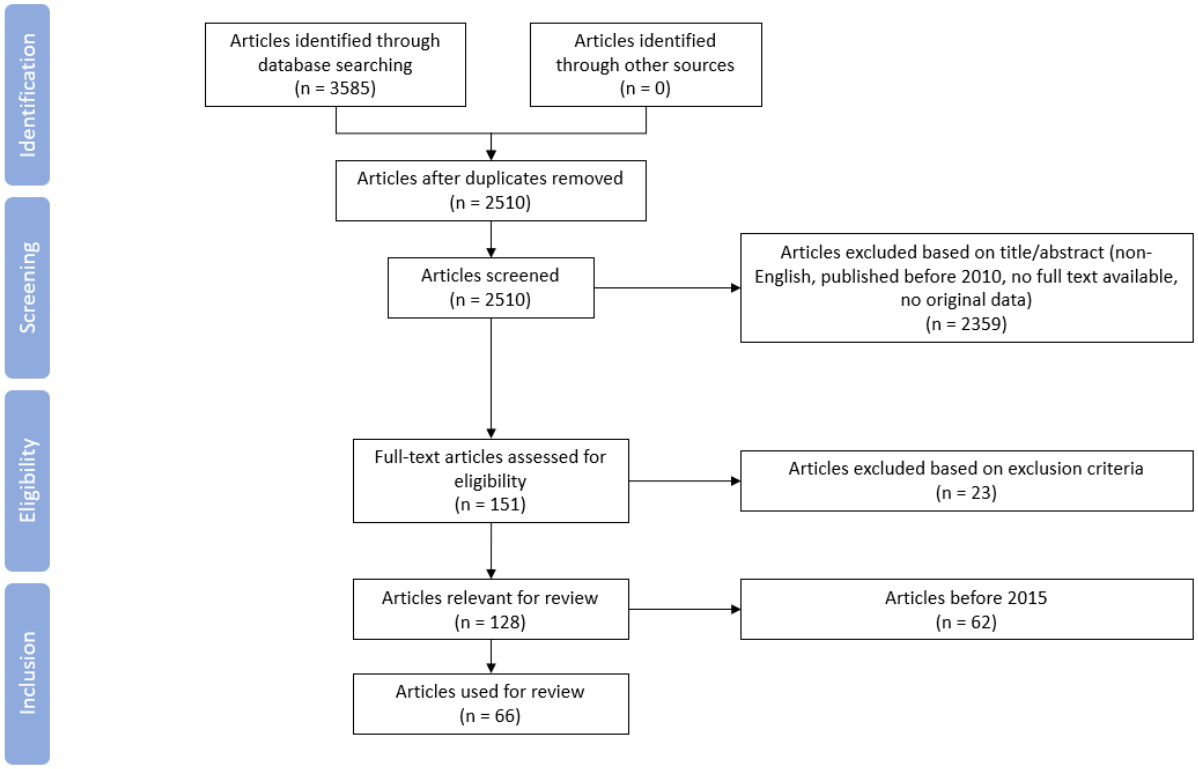

Figure 2. Flow chart summarizing study selection process

automated segmentation of small vessels in soft tissue.

Methods

This systematic review was performed according to the PRISMA guidelines (16).

Search Strategy

On March 23rd 2021, a systematic search was conducted using several databases: Embase, Medline ALL (Ovid), Web of Science Core Collection, Cochrane and Google Scholar. The search strings can be found in Appendix I.

Eligibility Selection

The articles found by this search were checked for duplicates and scanned for eligibility. Two independent authors performed the selection based on inclusion and exclusion criteria. Articles that were not agreed upon, were further discussed between the authors until consensus was reached.

Studies on soft tissue imaged using computed tomography angiography (CTA) or magnetic resonance angiography (MRA), vessel segmentation method as primary study subject and a clinical application for the segmentation method were included for this systematic review. Non-human studies, studies published before 2015, studies not published in English and of which no full text was available and not original data were excluded from this systematic review.

Outcome Measures

Each article was evaluated for imaging technique, anatomical region, image processing technique, size of the segmented vessels, extent of required manual input and translation to XR application. Image processing techniques were described by the segmentation model and image features used for the segmentation and the segmentation result (17). Additionally, performance evaluation metrics and results, validation and training dataset and the ground truth for

performance evaluation of the segmentation technique were assessed.

Results

Literature Search

The literature search resulted in 3585 articles, 2510 of which remained after duplicate removal. Of these remaining 2510 articles, 2359 articles were excluded based on title and abstract screening. The remaining 151 articles were fully read and 23 articles were excluded. Although 128 articles were considered suitable for review, 62 articles were written before 2015 and thus excluded for this review. 66 articles remained eligible for review. Figure 1 summarizes the study selection process.

Table 1. Study characteristics: authors, year, imaging modality, anatomical region, high level image processing technique. Active Contours = AC, Boundary Propagation = BP, Centerline = CE, Deep Learning = DL, Edge-Based = EB, Fuzzy Connectedness = FC, Geometry-Based = GB, Graph-Cut = GC, Geometry = GT, Intensity = IT, Level-Sets = LS, Lumen = LU, Machine Learning = ML, Outer Wall = OW, Region-Based = RB, Region Growing = RG, Statistical Model = SM.

Authors	Year	Imaging Modality	Anatomical Region	Image Processing (model | features | result)
Zhou et al. (18)	2021	CT	Carotid	DL | 3D U-Net CNN (CarotidNet) | LU
Gu et al. **(19)**	2021	CT	Gastrocolic	RB | IT | LU
Zhang et al. (20)	2020	MR	Intracranial	DL | 3D CNN | LU
Wang et al. (21)	2020	MR	Renal	RB | GC, IT & GT | CE
Tsakanikas et al. (22)	2020	MR	Carotid	DL | U-Net & AC | LU & OW
Tetteh et al. (23)	2020	MR	Intracranial	DL | 3D CNN (DeepVesselNet) | CE
Quon et al. (24)	2020	MR	Intracranial	DL | 2D U-Net CNN | LU
(Nazir et al. (25)	2020	CT	Intracranial	DL | Fully 3D E2E Network | LU
Mavioso et al. (1)	2020	CT	Deep Inferior Epigastric Artery Perforator	RB| IT Tracking & Cost | CE
Leonardi et al. **(26)**	2020	MR	Aorta	GB | IT & GT | LU
Ivashchenko et al. (27)	2020	MR	Hepatic	RB | IT Tresholding| CE & LU
Guo et al. (28)	2020	CT	Hepatic	RB | GC, IT Tracking & Cost| CE & LU
Fu et al. (29)	2020	CT	Intracranial/ carotid	DL | 3D CNN (CerebralDoc)| LU
Fantazzini et al. **(30)**	2020	CT	Aorta	DL | 2D CNN | LU
Zhao et al. (31)	2019	MR	Intracranial	DL | Multi-Layer NN | LU
Zhang et al. (32)	2019	CT	Pulmonary	RB | IT Tracking & FC | LU
Zhai et al. **(33)**	2019	CT	Pulmonary	RB | GC, IT | LU

Wolterink et al. **(34)**	2019	CT	Coronary	DL | 3D CNN | CL
Wang et al. (35)	2019	MR	Carotid	EB | LS, IT | LU
Torrents-Barrena et al. (36)	2019	MR	Placenta	GB | Curvature Detection & Morphology| LU
Tahoces et al. **(37)**	2019	CT	Aorta	RB | GT Tracking & Cost | CE & LU
Sukanya et al. (38)	2019	CT	Coronary	RB | IT & Gradient | Vessel enhancement
Sedghi Gamechi et al. (39)	2019	CT	Aorta	RB | GC & Cost | CL
Oda et al. (40)	2019	CT	Abdominal	DL | 2D U-Net FCN | LU
Neumann et al. (41)	2019	MR	Intracranial	RB | LS, IT | LU
Luzon et al. **(42)**	2019	CT	Mesenteric	EB | AC | LU
Liu et al. (43)	2019	CT	Coronary	RB | LS, IT & Cost | CE & LU
Lebre et al. (44)	2019	CT/MR	Hepatic	RB | IT & GT | CE & LU
Lareyre et al. (45)	2019	CT	Aorta	EB | AC & BP | LU
Kitrungrotsakul et al. **(46)**	2019	MR	Hepatic	DL | 3D CNN (VesselNet) | LU
Kahala et al. (47)	2019	MR	Breast	RB | IT | CE
Hernandez-Delgado et al. (48)	2019	MR	Full Body	RB | IT & FC | LU
El Hadji et al. (49)	2019	CT	Intracranial	DL | FCNN | LU
Gu et al. (50)	2019	CT	Pulmonary	DL | FCNN | LU
Duan et al. (51)	2019	CT	Pulmonary	RB | IT & RG | LU
Zhu et al. (52)	2018	CT	Intracranial	GB | GT | CL
Zhang et al. (53)	2018	CT	Hepatic	RB | IT Thresholding & FC | LU
Zeng et al. **(54)**	2018	CT	Hepatic	RB | RG & AC/clustering | LU
Phellan et al. (55)	2018	MR	Intracranial	RB | IT & Seed-Based | LU
Deng et al. (56)	2018	CT	Aorta	RB | GC, IT | LU
Chung et al. (57)	2018	CT	Hepatic	RB | Morphology & AC | LU
Bozkurt et al. **(58)**	2018	CT	Carotid	RB | RG, Seed Tracking | CE & LU

Arias-Lorza et al. (59)	2018	MR	Carotid	RB | IT, Cost Path | CE
Zeng et al. (60)	2017	CT	Hepatic	RB | Fast Marching, GC | CE & LU
Xiao et al. (61)	2017	MR	Intracranial	RB | IT & GT | LU
Selvalakshmi et al. (62)	2017	CT	Hepatic	RB | AC, FC | LU
Lidayová et al. (63)	2017	CT	Femoral	GB | IT, GT | CE & LU
Hsu et al. (64)	2017	MR	Intracranial	RB | IT, Fast Marching, AC | CE & LU
Gao et al. **(65)**	2017	MR	Carotid	EB | Edge-Detection, Model-Fitting | LU & OW
Ali et al. (66)	2017	CT	Full Body	RB | LS, IT | LU
Zeng et al. (67)	2016	CT	Hepatic	ML | IT | LU
Wang et al. (68)	2016	MR	Intracranial	RB | IT, Cost | LU
Wang et al. (69)	2016	MR	Intracranial	RB | IT, Cost | LU
Volonghi et al. **(70)**	2016	MR	Aorta	RB | LS, Marching Cubes | LU
Selver et al. (71)	2016	CT/MR	Aorta	GB | Cost Path | LU
Lu et al. **(72)**	2016	CT/MR	Full Body	SM | IT, MAP-Markov | LU
Jang et al. (73)	2016	CT	Aorta	GB | Seed Points, Energy | LU
Gao et al. (74)	2016	CT	Femoral	RB | Deformable Model | CE & LU
Cao et al. (75)	2016	MR	Intracranial	SM | Markov & PSO | LU
Wen et al. **(76)**	2015	MR	Intracranial	RB | IT, PSO | CE & LU
Wang et al. **(77)**	2015	MR	Intracranial	RB | IT Thresholding | LU
Ukwatta et al. (78)	2015	MR	Femoral	GB | Convex Optimization | LU & OW
Hemmati et al. **(79)**	2015	CT	Carotid	RB | IT, Minimum Path, LS | CE & LU
Guo et al. (80)	2015	CT	Hepatic	RB | IT, Adaptive Threshold | LU
Fabijanska (81)	2015	CT	Pulmonary	RB | Random Walk seeds, 3D RG | LU
Chen et al. (82)	2015	MR	Femoral	RB | Deformable model | LU & OW

Study Characteristics

The included articles were published between 2015 and 2021. Each article covered a BVS technique for at least one anatomical region. The study characteristics are presented in Table 1.

The main anatomical regions studied were the intracranial and liver vessels and the aorta. 17 articles presented a segmentation method of the intracranial vascular structure, 11 articles presented a segmentation method of the hepatic vasculature and 9 articles presented a segmentation method for the

aorta. The other anatomical regions were the pulmonary (32, 33, 50, 51, 81), carotid (18, 22, 35, 58, 59, 65, 79), general abdominal (40), mesenteric (42), gastrocolic (19), renal (21), placenta (36), breast (47), coronary (34, 38, 43), femoral (63, 74, 78, 82) and full body/not specified (48, 66, 72) vasculature. One article presented a segmentation method of DIEAP vessels specifically (1).

CT imaging was used as a base for 36 articles. 27 articles used MR imaging as a base for segmentation. 3 articles were not specific on the imaging modality but mentioned both MR and CT (44, 71, 72).

Applicability for Automated (Super)microvessel Segmentation

The size of the segmented vessels and their need for manual input are presented in Table 2. The exact vessel size was not mentioned in any of the articles. Therefore, reference papers were used and the sizes mentioned in this article are estimations.

29 articles presented a method for segmentation of an anatomical region where the smallest vessels would be classified as supermicrovessels. Only one article presented a method where the full vessel range was classified as supermicrovessels (36). Additionally, six articles presented a method for segmentation of an anatomical region where the smallest vessels would be classified as microvessels (32, 33, 50, 51, 63, 81) and one article presented a method where the full vessel range was classified as microvessels (1). In three articles, the vessel size or anatomical region was not defined (48, 66, 72).

The majority of methods was fully automatic, 12 articles required user input for their BVS method. Two articles did not mention whether user input was required (38, 48).

Evaluation Metrics, Ground Truth and Datasets

The performance evaluation results, validation dataset and ground truth for comparison are presented in Table 2. The majority of the segmentation methods used a clinical dataset for training their algorithm. In addition to a clinical dataset, four articles also used a synthetic dataset for training their algorithm (23, 46, 53, 54) and two articles used phantoms in addition to a clinical dataset (33, 64). One article used a synthetic dataset for training their algorithm (66).

The evaluation metrics differ per article. The Dice Similarity Coefficient (DSC), Hausdorff Distance (HSD), Accuracy (ACC), Sensitivity (SENS) and Specificity (SPEC) were the most frequently used evaluation metrics. In five articles, the evaluation metrics were not mentioned (19, 62, 64, 72, 80). In two articles, the metrics were mentioned but their results were not elucidated (59, 75). 17 methods used one or more external datasets for validation of their methods. The majority of articles used manual segmentation as their ground truth. In addition to a manually produced ground truth, one article used commercially available software (73). One article used synthetic data as ground truth (21), one used a phantom (72), two articles used prior methods (38, 64) and three articles did not discuss their ground truth (19, 62, 66). One article did not discuss their used evaluation metric, ground truth or validation datasets (19).

Applicability for Extended Reality

The possibility for translation of vessel segmentation to XR was not researched by the articles included in this research.

Table 2. Article specifics regarding clinical results, to which extent the method is automated and vessel size. Note: vessel size was not mentioned in any of the articles and therefore reference papers were used.
Data/Validation: Clinical Dataset = CL, External Dataset = EX, Fully automated = FA, Internal Dataset = IN, Manual Segmentation = MS, Not Disclosed = ND, Phantom = PH, Semi-automated = SA, Synthetic Dataset = SY.
Performance Evaluation Results: Accuracy = ACC, Area Overlap = AO, Area Under Curve = AUC, Dice Similarity Coefficient = DSC, False Negative Rate = FNR, False Positive Rate = FPR, Hausdorff Distance = HSD, Intra-Class Correlation = ICC, Jaccard Index = JAC, Kappa's statistic = KAP, Mean Absolute Distance = MAD, Maximum Distance = MAXD, Mean Euclidean Distance = MED, Mean Surface Distance = MSD, Positive Predictive Value = PPV, Precision = PREC, Peak Signal-to-Noise Ratio = PSNR, Recall = REC, Root Mean Square = RMS, Root Mean Square Surface Distance = RMSSD, Sensitivity = SENS, Similarity = SIM, Specificity = SPEC, Volumetric Similarity = VS.

Authors	**Training Data**	**User Input**	**Vessel size**	**Extended Reality**	**Performance Evaluation Results**	**Validation**	**Ground truth**
Zhou et al. (18)	CL	FA	4.3-7.7 mm (83)	ND	DSC 82.26% MSD 0.68 mm HSD 7.54 mm	EX | CL (MICCAI, 2009)	MS
Gu et al. (19)	CL	SA	3.5 mm (84)	ND	ND	ND	ND
Zhang et al. (20)	CL	FA	0.8-4.3 mm (85)	ND	DSC 93.2% PPV 96.5% SENS 90.1% ACC 99.9%	EX | CL (MIDAS) (86)	MS
Wang et al. (21)	CL	FA	4.2-5.5 mm (87)	ND	Centerline Overlap 84.0% Centerline Error 1.37 mm	IN | CL/SY	SY
Tsakanikas et al. (22)	CL	FA	4.3-7.7 mm (83)	ND	HSD 2.71mm ± 1.2	IN | CL	MS
Tetteh et al. (23)	CL/SY	FA	0.8-4.3 mm (85)	ND	PREC 86.44% REC 86.93% DSC 86.68%	IN | CL	MS
Quon et al. (24)	CL	FA	0.8-4.3 mm (85)	ND	DSC 75%	IN | CL	MS
Nazir et al. (25)	CL	FA	0.8-4.3 mm (85)	ND	DSC 90.8% HSD 5.01 mm PPV 89.6% Absolute Volumetric Difference 87.9%	IN | CL	MS
Mavioso et al. (1)	CL	SA	0.3-1.5 mm (88)	ND	Paired t-test 0.44	IN | CL	MS
Leonardi et al. (26)	CL	FA	13.4-20.4mm (89)	ND	Point-to-mesh distance 3.0 mm ± 0.58	EX | CL (Sim-e-Child) (90)	MS
Ivashchenko et al. (27)	CL	FA	0.6-7.3 mm (91)	ND	HSD_{broad} 1.2 mm ± 2.0 HSD_{narrow} 0.6 mm ± 0.8	IN | CL	MS

Guo et al. (28)	CL	FA	0.6-7.3 mm (91)	ND	ACC 97.8% SENS 66.2% SPEC 98.7%	EX | CL (3Dircadb) (92)	MS
Fu et al. (29)	CL	FA	0.8-7.7 mm (83, 85)	ND	DSC 94.4% Vessel score -0.93 REC 93.3%	EX | CL	MS
Fantazzini et al. (30)	CL	FA	13.4-20.4mm (89)	ND	DSC 92.8% JAC 86.6% MSD 0.71 mm ± 0.64 MAXD 50.1 mm ± 37.3	IN | CL	MS
Zhao et al. (31)	CL	FA	0.8-4.3 mm (85)	ND	ACC 94.8% SENS 0.7826 SPEC 0.9866 PREC 0.931 DSC 85.0%	EX | CL (MIDAS) (86)	MS
Zhang et al. (32)	CL	FA	1.0-30 mm (93)	ND	DSC 92.2% SIM 0.9097 SENS 0.9036 PREC 0.9432	IN | CL	MS
Zhai et al. (33)	CL/PH	FA	1.0-30 mm (93)	ND	AUC 0.976	EX | CL (VESSEL12)	MS
Wolterink et al. (34)	CL	FA	2.1-4.1 mm (94)	ND	Total overlap 93.7% Overlap to first error 81.5% Clin. Relevant overlap 97.0% Inner ACC 0.21mm	EX | CL (MICCAI, 2008)	MS
Wang et al. (35)	CL	SA	4.3-7.7 mm (83)	ND	DSC 89.1% PSNR 27.36 HSD 17.2mm ± 6.9 Mean Sum Square Dist (MSSD) 7.4 mm ± 5.5	IN | CL	MS
Torrents-Barrena et al. (36)	CL	FA	0.1-0.3 mm (95)	ND	HSD 44.06 mm ± 16.01 AUC 0.86 SENS 0.75 SPEC 100% PREC 0.93 ACC 100% DSC 81% JAC 73%	IN | CL	MS
Tahoces et al. (37)	CL	FA	13.4-20.4mm (89)	ND	DSC 95.1%	EX | CL (LIDC) (96)	MS
Sukanya et al. (38)	CL	ND	2.1-4.1 mm (94)	ND	PSNR 5.89 Entropy 4.33 Structural Similarity Index Matrix 0.046	IN | CL	Frangi's Vessel-ness (97)

Sedghi Gamechi et al. (39)	CL	FA	13.4-20.4mm (89)	ND	DSC 95% MSD 0.56 mm ± 0.08 MAD 2.55 mm ± 1.94	IN | CL	MS
Oda et al. (40)	CL	FA	13.4-20.4mm (89)	ND	DSC 87.1% PREC 86.1% REC 89.0%	IN | CL	MS
Neumann et al. (41)	CL	FA	0.8-4.3 mm (85)	ND	DSC 86.9% Matthews Correlation Coefficient 86.7% KAP 0.867 ICC 0.868	IN | CL	MS
Luzon et al. (42)	CL	SA	4.0-8.0 mm (98)	ND	RMS 1.20 mm ± 0.82 MED 2.14 mm ± 1.60	IN | CL	MS
Liu et al. (43)	CL	FA	2.14-4.12 mm (94)	ND	DSC 83.4%	IN | CL	MS
Lebre et al. (44)	CL	FA	0.6-7.3 mm (91)	ND	DSC 93% REC 0.92 PREC 0.94 JAC 87%	EX | CL (SLIVER & IRCAD) (99, 100)	MS
Lareyre et al. (45)	CL	FA	13.4-20.4mm (89)	ND	DSC 93% Mean VS 0.96 SENS 0.90 SPEC 0.93 JAC 87% HSD 1.77 mm ± 0.38	IN | CL	MS
Kitrungrotsakul et al. (46)	CL/SY	FA	0.6-7.3 mm (91)	ND	DSC 90.3% Volumetric Overlap Error 17.2% SENS 0.929 PPV 0.842	EX | CL/SY (IRCAD & VASCUSYNTH) (99, 101)	MS
Kahala et al. (47)	CL	FA	0.5-4.8 mm (102)	ND	SENS 0.86 SPEC 0.883	IN | CL	MS
Hernandez et al. (48)	CL	ND	ND	ND	SENS 0.674 SPEC 0.988 ACC 0.976	IN | CL	MS
El Hadji et al. (49)	CL	FA	0.8-4.3 mm (85)	ND	DSC 79% PREC 0.8 REC 0.69	IN | CL	MS
Gu et al. (50)	CL	FA	1.0-30 mm (93)	ND	DSC 94.1% JAC 89.0% VS 0.991	IN | CL	MS
Duan et al. (51)	CL	FA	1.0-30 mm (93)	ND	SENS 92.9% SPEC 91.6% AUC 0.972	EX | CL (VESSEL12)	MS
Zhu et al. (52)	CL	SA	0.8-4.3 mm (85)	ND	Average Distance 1.65 mm ± 2.95	EX | CL (MIDAS) (86)	MS

Zhang et al. (53)	CL/SY	FA	0.6-7.3 mm (91)	ND	DSC 67.3% (3Dircabd), 71.4% (SLIVER) ACC 96.4% (3Dircabd), 96.8% (SLIVER) SENS 73.7% (3Dircabd), 97.6% (SLIVER) SPEC 97.4% (3Dircabd), 97.6% (SLIVER)	EX | CL/SY (3Dircadb & SLIVER & VASCUSYNTH) (92)	MS
Zeng et al. (54)	CL/SY	FA	0.6-7.3 mm (91)	ND	DSC 73.0% JAC 66.1% ACC 0.981 SENS 0.683 SPEC 0.992 RMS Distance 2.56 mm	IN/EX | CL/SY (VASCUSYNTH) (97)	MS
Phellan et al. (55)	CL	FA	0.8-4.3 mm (85)	ND	DSC 96.8%	IN | CL	MS
Deng et al. (56)	CL	FA	13.4-20.4mm (89)	ND	DSC 96.9% HSD 4.6 mm	IN | CL	MS
Chung et al. (57)	CL	FA	0.6-7.3 mm (91)	ND	DSC 96%	IN | CL	MS
Bozkurt et al. (58)	CL	FA	4.3-7.7 mm (83)	ND	DSC 92.8% MSD 0.16 mm RMSSD 0.24 HSD 1.72 mm ACC 99%	EX/IN | CL (MICCAI, 2009)	MS
Arias-Lorza et al. (59)	CL	FA	4.3-7.7 mm (83)	ND	HSD ND Centerline Artery Distance ND	EX | CL (ROTTERDAM study) (103)	MS
Zeng et al. (60)	CL	FA	0.6-7.3 mm (91)	ND	ACC 0.977 SENS 0.798 SPEC 0.986	IN | CL	MS
Xiao et al. (61)	CL	FA	0.8-4.3 mm (85)	ND	DSC 82.2% FPR 0.249 FNR 0.127	IN | CL	MS
Selvalakshmi et al. (62)	CL	SA	0.6-7.3 mm (91)	ND	ND	IN | CL	ND
Lidayová et al. (63)	CL	FA	<1.5-20.4 mm (63, 89)	ND	Overlap rate 100% Detection rate 59.45 %	IN | CL	MS
Hsu et al. (64)	CL/PH	FA	0.8-4.3 mm (85)	ND	ND	IN | CL/PH	Prior filters

Gao et al. (65)	CL	SA	4.3-7.7 mm (83)	ND	DSC 92% LU, 90% OW MAXD 0.56 ± 0.22 LU, 1.19 ± 0.49 OW RMSED 0.26 ± 0.1 LU. 0.52 ± 0.21 OW Degree of Similarity 92.7% LU, 67.0% OW	IN | CL	MS
Ali et al. (66)	SY	FA	ND	ND	Mean Square Error 0.0019 PSNR 27.1 JAC 43.9%	IN | SY	ND
Zeng et al. (67)	CL	FA	0.6-7.3 mm (91)	ND	ACC 98.1% SENS 74.2% SPEC 99.3%	IN | CL	MS
Wang et al. (68)	CL	FA	0.8-4.3 mm (85)	ND	DSC 90.13%	IN | CL	MS
Wang et al. (69)	CL	FA	0.8-4.3 mm (85)	ND	DSC 90.13%	IN | CL	MS
Volonghi et al. (70)	CL	FA	13.4-20.4mm (89)	ND	DSC 91% Average Symmetric Distance 1.09 mm RMSSD 1.58 mm	IN | CL	MS
Selver et al. (71)	CL	SA	13.4-20.4mm (89)	ND	Average SSD 0.11 mm ± 1.56 Mean SSD 0.46 mm ± 0.08 DSC 82.68% JAC 80.54% SE 83.7%	IN | CL	MS
Lu et al. (72)	CL/PH	FA	ND	ND	ND	IN | CL/PH	PH
Jang et al. (73)	CL	FA	13.4-20.4mm (89)	ND	DSC 94.98%	IN | CL	MS & Vitrea (104)
Gao et al. (74)	CL	FA	2.5-9.6 mm (105)	ND	Average RMS Error 2.55 mm ± 0.7 Average Mean Error 1.63 mm ± 0.4 DSC >95.2%	IN | CL	MS
Cao et al. (75)	CL	FA	0.8-4.3 mm (85)	ND	DSC ND JAC ND	IN | CL	MS
Wen et al. (76)	CL	FA	0.8-4.3 mm (85)	ND	# Vessel Pixels	IN | CL	MS
Wang et al. (77)	CL	FA	0.8-4.3 mm (85)	ND	DSC 84% FPR 0.07 FNR 0.22	IN | CL	MS

Ukwatta et al. (78)	CL	SA	2.5-9.6 mm (105)	ND	DSC 90.9% OW, 87.8% LU AO 83.9% OW, 80.2% LU MAD 0.36 mm ± 0.18 OW, 0.34 ± 0.15 LU MAXD 0.91 mm ± 0.33 OW, 0.85 mm ± 0.47	IN | CL	MS
Hemmati et al. (79)	CL	SA	4.3-7.7 mm (83)	ND	DSC 85% Mean Absolute Surface Distance 0.42 mm	IN | CL	MS
Guo et al. (80)	CL	SA	0.6-7.3 mm (91)	ND	ND	IN | CL	MS
Fabijanska (81)	CL	FA	1.0-30 mm (93)	ND	SENS 0.9 SPEC >0.9 DSC ~ 91%	EX | CL (EXACT, 2009) (106)	MS
Chen et al. (82)	CL	SA	2.5-9.6 mm (105)	ND	MAD 0.28 mm LU, 0.315 mm OW MAXD 0.625 mm LU, 0.65 OW AO 80% LU, 84.7% OW Average Distance 5.9% LU, 8.5% OW DSC 88.2% LU, 91.7% OW	IN | CL	MS

Discussion

In DIEAP flap autologous breast reconstruction, the donor site involves (super)microvessels in soft tissues. To improve the preoperative imaging for these reconstructions and accommodate 3D visualization, an adequate segmentation of these structures is essential. This systematic review assessed BVS techniques for small vessels in soft tissues from 2015-2021. In recent years, many articles have described various methods for BVS. Considering automated (super)microvessel segmentation for 3D visualization of the DIEAP flap preoperative planning, several findings from this study are remarkable.

Segmentation Comparison and Quality

We found 31 articles studying vessels that could be defined as (super)microvessels. The performance evaluation of BVS methods is difficult to compare due to a limited standardization in evaluation metrics. For some fields, such as coronary, intracranial and pulmonary vessel segmentation, challenges have been set up to create more standardized evaluation framework (https://grand-challenge.org/). This allows for inter-algorithm comparison between studies within one challenge framework. However, not all studies use these challenge frameworks.

The variety in performance evaluation measures in the articles included in this review makes conducting a proper meta analysis impossible. To compare the methods, we used the ground truth and the datasets used for training and validation of the segmentation techniques. The golden standard for a ground truth is manual segmentation by a clinical expert. In case of an artificial intelligence (AI) segmentation technique, the algorithm trains on the ground truth. In an algorithm without AI, the algorithm is manually improved based on the ground truth. To avoid overtraining on one dataset and making your algorithm

inapplicable to other datasets, the training and validation datasets need to be different. Using a separate or an external dataset (e.g. a challenge framework) for validation of an algorithm is more robust than using the same dataset for training and testing.

Automated Segmentation for DIEAP Vessels for Clinical Use

Although only few require manual user input and BVS is an important aspect of 3D visualization of preoperative planning, there are no methods directly applicable for segmentation of small vessels in DIEAP flaps donor site imaging. The calibre of DIEAP vessels generally ranges between 1.00 and 3.49 mm. The corresponding venous calibre generally ranges from 0.50 to 4.32 mm. The combined difficulty of tiny vessels and low contrast to their surrounding tissue makes adoption of an automatic algorithm developed for another anatomical region complicated.

29 articles report the ability to segment supermicrovessels, mainly the distal vessels of the intracranial and hepatic vasculature. Of these 29 articles, three were semi-automated and 26 were fully automatic segmentation methods. Zhang et al. (20) present a promising DL method for automatic segmentation of intracranial vessels, validated by an external dataset. Lebre et al. (44) present a fully automatic method for segmentation of the hepatic vasculature, which yields promising results after validation with an external database. Mavioso et al. (1) present the only method developed for segmentation of DIEAP vessels, resulting in a centerline segmentation. However, their method is semi-automated, does not make use of the most-used performance evaluation metrics and is not validated by an external dataset. Torrents-Barrena et al. (36) present an automated method for segmentation of vessels of the placenta. Their method provides a fully automatic lumen segmentation of the placenta vasculature. The method developed by Wang et al. (21) for automatic renal vasculature segmentation does not cover the segmentation of (super)microvessels, but the lack of contrast in their anatomical site may also be applicable to DIEAP vessel segmentation. However, their used ground truth is a synthetic dataset.

Despite being trained and validated on clinical datasets, none of the segmentation methods found in this review are directly ready for use in clinical practice. Good performance results for segmentations are not directly interchangeable between different anatomical regions. This is mainly due to differences in surrounding tissues and variances in imaging modality. The in-plane spatial resolution of a CTA ranges from 0.50-0.625 mm. CT slice thickness can vary, but decreasing slice thickness increases image noise, making small structures difficult to distinguish. The spatial resolution of an MRA is inferior to that of a CTA, typically 1-2 mm (10, 11, 107). However, MRA images generally show better contrast between soft tissues.

In addition to the anatomical and imaging differences, the proposed segmentation methods are initialized from a script separate from the clinical practice. They are research oriented and do not have a user interface. For implementation in clinical practice, a BVS method for small vessels in low-contrast soft tissues would have to be integrated into the clinical workflow, e.g. by integration in the Picture Archiving and Communication System (PACS) or being accessible from the PACS with an intuitive user interface.

Further Research

For this review, we have included articles published from 2015 on. Older methods were not included because they have been replaced, updated and/or improved by more

recent methods. In many recent articles, DL and ML techniques are used for BVS. These techniques generally have a superior performance compared to older algorithms, although they depend on the availability of (large) annotated datasets for training their models. For some anatomical regions, large databases are available for DL purposes. An unavailability of these large annotated ground base datasets makes DL difficult to implement for segmentation of DIEAP vessels. As DL approaches show promising results, for further research it would be interesting to investigate the viability of sharing data between medical centres and establishing a database for DIEAP vessels.

Initially, we proposed a study on the use of AI for BVS and its translation to a 3D XR environment for improvement of preoperative planning. An interesting finding from this review, is the fact that none of the included articles covered a translation of BVS to and XR environment. However, several studies mention segmentation for 3D visualization on a 2D screen. This indicates that there is a gap between studies in other fields indicating that a preoperative planning in an XR environment could be beneficial and our field of interest. For further research, it would be interesting to explore the benefits of 3D visualization of a BVS on 2D screens or in an XR environment on preoperative planning.

Conclusion

This systematic review provides an overview of recent advancements in blood vessel segmentation techniques with a specific interest in (super)microvessels. Although there are many methods available for automated segmentation of small vessels and one for semi-automated segmentation of DIEAP vessels specifically, the research is still a long way from application in clinical practice. For application to the DIEAP vessels and useability in 3D visualization in clinical practice, further research will need to be conducted. Future works can include testing the performance of promising fully automated methods on small vessels with low contrast, investigating the importance of vessel segmentation for 3D visualization of preoperative planning and evaluating the clinical benefit of improving preoperative planning for DIEAP flap autologous breast reconstructions.

References

1. Mavioso C, Araújo RJ, Oliveira HP, Anacleto JC. Automatic detection of perforators for microsurgical reconstruction: Elsevier; 2020.
2. Essert C, Joskowicz L. Image-based surgery planning. In: S. Kevin Zhou DR, Gabor Fichitinger, editor. Handbook of Medical Image Computing and Computer Assisted Intervention: Elsevier; 2020. p. 795-815.
3. Hamdi M, Rebecca A. The Deep Inferior Epigastric Artery Perforator Flap (DIEAP) in Breast Reconstruction. Semin Plast Surg. 2006;20(2):95-102.
4. Rajan S. Uppal BC, Koendaar Van Landuyt, Phillip Blondeel. The efficacy of preoperative mapping of perforators in reducing operative times and complications in perforator flap breast reconstruction. Journal of Plastic, Reconstructive & Aesthetic Surgery. 2008;62:859-64.
5. Sadeghi AH, Bakhuis W, Van Schaagen F, Oei FBS, Bekkers JA, Maat APWM, et al. Immersive 3D virtual reality imaging in planning minimally invasive and complex adult cardiac surgery. European Heart Journal - Digital Health. 2020;1(1):62-70.
6. Timonen T, Iso-Mustajärvi M, Linder P, Lehtimäki A, Löppönen H, Elomaa A-P, et al. Virtual reality improves the accuracy of simulated preoperative planning in temporal bones: a feasibility and validation study. European Archives of Oto-Rhino-Laryngology. 2020.
7. Pratt P, Ives M, Lawton G, Simmons J, Radev N, Spyropoulou L, et al. Through the HoloLens™ looking glass: augmented reality for extremity reconstruction surgery using 3D vascular models with perforating vessels. European Radiology Experimental. 2018;2(1):2.
8. Boedecker C, Huettl F, Saalfeld P, Paschold M, Kneist W, Baumgart J, et al. Using virtual 3D-models in surgical planning: workflow of an immersive virtual reality application in liver surgery. Langenbeck's Archives of Surgery. 2021.
9. Liberatore M, Wagner W. Virtual, mixed, and augmented reality: a systematic review for immersive systems research. Virtual Reality. 2021:1-27.
10. Mavioso C, Araújo RJ, Oliveira HP, Anacleto JC, Vasconcelos MA, Pinto D, et al. Automatic detection of perforators for microsurgical reconstruction. The Breast. 2020;50:19-24.
11. Hong JA-O, Song S, Suh HSP. Supermicrosurgery: Principles and applications. (1096-9098 (Electronic)).
12. Kirbas C, Quek F. A review of vessel extraction techniques and algorithms. ACM Computing Surveys (CSUR). 2004.
13. Lesage D, Angelini ED, Bloch I, Funka-Lea G. A review of 3D vessel lumen segmentation techniques: Models, features and extraction schemes. Med Image Anal. 2009;13(6):819-45.
14. Moccia S, De Momi E, El Hadji S, Mattos LS. Blood vessel segmentation algorithms — Review of methods, datasets and evaluation metrics. Computer Methods and Programs in Biomedicine. 2018;158:71-91.
15. Zhao F, Chen Y, Hou Y, He X. Segmentation of blood vessels using rule-based and machine-learning-based methods: a review. Multimedia Systems. 2019.
16. Shamseer L, Moher D, Clarke M, Ghersi D, Liberati A, Petticrew M, et al. Preferred reporting items for systematic review and meta-analysis protocols (PRISMA-P) 2015: elaboration and explanation. BMJ : British Medical Journal. 2015;349:g7647.
17. Lesage D, Angelini E, Bloch I, Funka-Lea G. A review of 3D vessel lumen segmentation techniques: Models, features and extraction schemes. Medical Image Analysis. 2009;13:819-45.

18. Zhou T, Tan T, Pan X, Tang H, Li J. Fully automatic deep learning trained on limited data for carotid artery segmentation from large image volumes. Quant Imaging Med Surg. 2021;11(1):67-83.
19. Gu L, Wen S, Xu C, Zhu J, Liu P, Xu Q. Computed tomography angiography of gastrocolic vein trunk by morphological filtering technique in right colon cancer. Ther Clin Risk Manage. 2021;17:1-7.
20. Zhang B, Liu S, Zhou S, Yang J, Wang C, Li N, et al. Cerebrovascular segmentation from TOF-MRA using model- and data-driven method via sparse labels: Elsevier; 2020.
21. Wang C, Oda M, Hayashi Y, Yoshino Y, Yamamoto T, Frangi AF, et al. Tensor-cut: A tensor-based graph-cut blood vessel segmentation method and its application to renal artery segmentation. Med Image Anal. 2020;60:101623.
22. Tsakanikas VD, Siogkas PK, Mantzaris MD, Potsika VT, Kigka VI, Exarchos TP, et al. A deep learning oriented method for automated 3D reconstruction of carotid arterial trees from MR imaging. Annu Int Conf IEEE Eng Med Biol Soc. 2020;2020:2408-11.
23. Tetteh G, Efremov V, Forkert ND, Schneider M, Kirschke J, Weber B, et al. DeepVesselNet: Vessel Segmentation, Centerline Prediction, and Bifurcation Detection in 3-D Angiographic Volumes. Front Neurosci. 2020;14.
24. Quon JL, Chen LC, Kim L, Grant GA, Edwards MSB, Cheshier SH, et al. Deep Learning for Automated Delineation of Pediatric Cerebral Arteries on Pre-operative Brain Magnetic Resonance Imaging. Front surg. 2020;7:517375.
25. Nazir A, Cheema MN, Sheng B, Li H. Off-enet: An optimally fused fully end-to-end network for automatic dense volumetric 3d intracranial blood vessels segmentation. … on Image Processing. 2020.
26. Leonardi B, D'Avenio G, Vitanovski D, Grigioni M, Perrone MA, Romeo F, et al. Patient-specific three-dimensional aortic arch modeling for automatic measurements: Clinical validation in aortic coarctation. J Cardiovasc Med. 2020;21(7):517-28.
27. Ivashchenko OV, Rijkhorst EJ, Ter Beek LC, Hoetjes NJ, Pouw B, Nijkamp J, et al. A workflow for automated segmentation of the liver surface, hepatic vasculature and biliary tree anatomy from multiphase MR images. Magn Reson Imaging. 2020;68:53-65.
28. Guo X, Xiao R, Zhang T, Chen C, Wang J, Wang Z. A novel method to model hepatic vascular network using vessel segmentation, thinning, and completion. Med Biol Eng Comput. 2020;58(4):709-24.
29. Fu F, Wei J, Zhang M, Yu F, Xiao Y, Rong D, et al. Rapid vessel segmentation and reconstruction of head and neck angiograms using 3D convolutional neural network. Nat Commun. 2020;11(1):4829.
30. Fantazzini A, Esposito M, Finotello A, Auricchio F, Pane B, Basso C, et al. 3D Automatic Segmentation of Aortic Computed Tomography Angiography Combining Multi-View 2D Convolutional Neural Networks. Cardiovasc Eng Technol. 2020;11(5):576-86.
31. Zhao S, Tian Y, Wang X, Xie L, Sun L. Intracranial vascular structure extraction: a machine learning approach. IEEE Access. 2019.
32. Zhang C, Sun M, Wei Y, Zhang H, Xie S, Liu T. Automatic segmentation of arterial tree from 3D computed tomographic pulmonary angiography (CTPA) scans. Comput Assist Surg (Abingdon). 2019;24:79-86.
33. Zhai ZW, Staring M, Giron IH, Veldkamp WJH, Kroft LJ, Ninaber MK, et al. Automatic quantitative analysis of pulmonary vascular morphology in CT images. Medical Physics. 2019;46(9):3985-97.

34. Wolterink JM, Hamersvelt RWV, Viergever MA, Leiner T, Išgum I. Coronary artery centerline extraction in cardiac CT angiography using a CNN-based orientation classifier. Med Image Anal. 2019;51:46-60.
35. Wang Y, Kao E, Zhang Y, Tian B, Gong J, Faraji F, et al. Shape-appearance constrained segmentation and separation of vein and artery in pulsatile tinnitus patients based on MR angiography and flow MRI. Magn Reson Imaging. 2019;61:187-95.
36. Torrents-Barrena J, Piella G, Masoller N, Gratacos E, Eixarch E, Ceresa M, et al. Fully automatic 3D reconstruction of the placenta and its peripheral vasculature in intrauterine fetal MRI. Med Image Anal. 2019;54:263-79.
37. Tahoces PG, Alvarez L, González E, Cuenca C, Trujillo A, Santana-Cedrés D, et al. Automatic estimation of the aortic lumen geometry by ellipse tracking. Int J Comput Assisted Radiol Surg. 2019;14(2):345-55.
38. Sukanya A, Rajeswari R. A modified Frangi's vesselness measure based on gradient and grayscale values for coronary artery detection. Journal of Intelligent & Fuzzy Systems. 2019;37(2):2327-36.
39. Sedghi Gamechi Z, Bons LR, Giordano M, Bos D, Budde RPJ, Kofoed KF, et al. Automated 3D segmentation and diameter measurement of the thoracic aorta on non-contrast enhanced CT. Eur Radiol. 2019;29(9):4613-23.
40. Oda M, Roth HR, Kitasaka T, Misawa K, Fujiwara M, Mori K. Abdominal artery segmentation method from CT volumes using fully convolutional neural network. Int j comput assist radiol surg. 2019;14(12):2069-81.
41. Neumann JO, Campos B, Younes B, Jakobs M, Unterberg A, Kiening K, et al. Evaluation of three automatic brain vessel segmentation methods for stereotactical trajectory planning. Comput Methods Programs Biomed. 2019;182:105037.
42. Luzon JA, Stimec BV, Kumar R, Elle OJ, Edwin B, Ignjatovic D. Semi-automated vs. expert manual 3D reconstruction of central mesenteric vascular models. the surgeon's verdict. Surg Endosc. 2019;33(2):S531.
43. Liu L, Xu J, Liu Z. Automatic segmentation of coronary lumen based on minimum path and image fusion from cardiac computed tomography images. Cluster Computing-the Journal of Networks Software Tools and Applications. 2019;22:1559-68.
44. Lebre MA, Vacavant A, Grand-Brochier M, Rositi H, Abergel A, Chabrot P, et al. Automatic segmentation methods for liver and hepatic vessels from CT and MRI volumes, applied to the Couinaud scheme. Comput Biol Med. 2019;110:42-51.
45. Lareyre F, Adam C, Carrier M, Dommerc C, Mialhe C, Raffort J. A fully automated pipeline for mining abdominal aortic aneurysm using image segmentation. Sci Rep. 2019;9(1):13750.
46. Kitrungrotsakul T, Han XH, Iwamoto Y, Lin L, Foruzan AH, Xiong W, et al. VesselNet: A deep convolutional neural network with multi pathways for robust hepatic vessel segmentation. Comput Med Imaging Graph. 2019;75:74-83.
47. Kahala G, Sklair M, Spitzer H. Multi-scale Blood Vessel Detection and Segmentation in Breast MRIs. J Med Biol Eng. 2019;39(3):424-30.
48. Hernandez-Delgado J, Cruz-Aceves I, Cordova-Fraga T, Sosa-Aquino M, Cabrera RG. Processing of MRI Images Weighted in TOF for Blood Vessels Analysis: 3-D Reconstruction. Computacion Y Sistemas. 2019;23(1):109-14.
49. Hadji SE, Moccia S, Scorza D, Rizzi M, Cardinale F, Baselli G, et al. Brain-vascular segmentation for SEEG planning via a 3D fully-convolutional neural network. Conf Proc IEEE Eng Med Biol Soc. 2019;2019:1014-7.

50. Gu X, Wang J, Zhao J, Li Q. Segmentation and suppression of pulmonary vessels in low-dose chest CT scans. Med Phys. 2019;46(8):3603-14.
51. Duan HH, Su GQ, Huang YC, Song LT, Nie SD. Segmentation of pulmonary vascular tree by incorporating vessel enhancement filter and variational region-growing. J Xray Sci Technol. 2019;27(2):343-60.
52. Zhu C, Wang X, Chen S, Xia M, Huang Y, Pan X. Automatic centerline extraction of cerebrovascular in 4D CTA based on tubular features. Phys Med Biol. 2018;63(12):125014.
53. Zhang R, Zhou Z, Wu W, Lin CC, Tsui PH, Wu S. An improved fuzzy connectedness method for automatic three-dimensional liver vessel segmentation in CT images. J Healthc Eng. 2018;2018.
54. Zeng YZ, Liao SH, Tang P, Zhao YQ, Liao M, Chen Y, et al. Automatic liver vessel segmentation using 3D region growing and hybrid active contour model. Comput Biol Med. 2018;97:63-73.
55. Phellan R, Lindner T, Helle M, Falcao AX, Forkert ND. Automatic Temporal Segmentation of Vessels of the Brain Using 4D ASL MRA Images. IEEE Trans Biomed Eng. 2018;65(7):1486-94.
56. Deng X, Zheng Y, Xu Y, Xi X, Li N, Yin Y. Graph cut based automatic aorta segmentation with an adaptive smoothness constraint in 3D abdominal CT images. Neurocomputing. 2018;310:46-58.
57. Chung M, Lee J, Chung JW, Shin YG. Accurate liver vessel segmentation via active contour model with dense vessel candidates. Comput Methods Programs Biomed. 2018;166:61-75.
58. Bozkurt F, Kose C, Sari A. An inverse approach for automatic segmentation of carotid and vertebral arteries in CTA. Expert Systems with Applications. 2018;93:358-75.
59. Arias-Lorza AM, Bos D, van der Lugt A, de Bruijne M. Cooperative carotid artery centerline extraction in MRI. PLoS ONE. 2018;13(5):e0197180.
60. Zeng YZ, Zhao YQ, Tang P, Liao M, Liang YX, Liao SH, et al. Liver vessel segmentation and identification based on oriented flux symmetry and graph cuts. Comput Methods Programs Biomed. 2017;150:31-9.
61. Xiao R, Ding H, Zhai F, Zhao T, Zhou W, Wang G. Vascular segmentation of head phase-contrast magnetic resonance angiograms using grayscale and shape features. Comput Methods Programs Biomed. 2017;142:157-66.
62. Selvalakshmi VM, Devi SN. Segmentation and 3D visualization of liver, lesions and major blood vessels in abdomen CTA images. Biomed Res. 2017;28(16):7206-12.
63. Lidayová K, Frimmel H, Bengtsson E, Smedby Ö. Improved centerline tree detection of diseased peripheral arteries with a cascading algorithm for vascular segmentation. J Med Imaging. 2017;4(2).
64. Hsu CY, Schneller B, Alaraj A, Flannery M, Zhou XJ, Linninger A. Automatic recognition of subject-specific cerebrovascular trees. Magn Reson Med. 2017;77(1):398-410.
65. Gao S, Van 'T Klooster R, Kitslaar PH, Coolen BF, Van Den Berg AM, Smits LP, et al. Learning-based automated segmentation of the carotid artery vessel wall in dual-sequence MRI using subdivision surface fitting. Med Phys. 2017;44(10):5244-59.
66. Ali E, Abdou MAER, El Sayed A. Automatic vessel extraction using particle swarming optimization for 3d medical images. Curr Med Imaging Rev. 2017;13(4):471-7.
67. Zeng YZ, Zhao YQ, Liao M, Zou BJ, Wang XF, Wang W. Liver vessel

segmentation based on extreme learning machine. Phys Med. 2016;32(5):709-16.
68. Wang J, Zhao S, Liu Z, Tian Y, Duan F, Pan Y. An Active Contour Model Based on Adaptive Threshold for Extraction of Cerebral Vascular Structures. Comput math methods med. 2016;2016:6472397.
69. Wang J, Zhao S, Liu Z, Tian Y. Segmentation of cerebral vascular structures using an active contour model. … on Virtual Reality and …. 2016.
70. Volonghi P, Tresoldi D, Cadioli M, Usuelli AM, Ponzini R, Morbiducci U, et al. Automatic extraction of three-dimensional thoracic aorta geometric model from phase contrast MRI for morphometric and hemodynamic characterization. Magn Reson Med. 2016;75(2):873-82.
71. Selver MA, Kavur AE. Implementation and use of 3D pairwise geodesic distance fields for seeding abdominal aortic vessels. Int J Comput Assisted Radiol Surg. 2016;11(5):803-16.
72. Lu P, Xia J, Li Z, Xiong J, Yang J, Zhou S, et al. A vessel segmentation method for multi-modality angiographic images based on multi-scale filtering and statistical models. Biomed Eng Online. 2016;15(1).
73. Jang Y, Jung HY, Hong Y, Cho I, Shim H, Chang HJ. Geodesic distance algorithm for extracting the ascending aorta from 3D CT images. Comp Math Methods Med. 2016;2016.
74. Gao X, Kitslaar PH, Budde RP, Tu S, de Graaf MA, Xu L, et al. Automatic detection of aorto-femoral vessel trajectory from whole-body computed tomography angiography data sets. Int J Cardiovasc Imaging. 2016;32(8):1311-22.
75. Cao RF, Wang XC, Wu ZK, Zhou MQ, Liu XY. A parallel Markov cerebrovascular segmentation algorithm based on statistical model. Journal of Computer …. 2016.
76. Wen L, Wang X, Wu Z, Zhou M, Jin JS. A novel statistical cerebrovascular segmentation algorithm with particle swarm optimization. Neurocomputing. 2015;148:569-77.
77. Wang R, Li C, Wang J, Wei X, Li Y, Zhu Y, et al. Threshold segmentation algorithm for automatic extraction of cerebral vessels from brain magnetic resonance angiography images. J Neurosci Methods. 2015;241:30-6.
78. Ukwatta E, Yuan J, Qiu W, Rajchl M, Chiu B, Fenster A. Joint segmentation of lumen and outer wall from femoral artery MR images: Towards 3D imaging measurements of peripheral arterial disease. Med Image Anal. 2015;26(1):120-32.
79. Hemmati H, Kamli-Asl A, Talebpour A, Shirani S. Semi-automatic 3D segmentation of carotid lumen in contrast-enhanced computed tomography angiography images. Phys Med. 2015;31(8):1098-104.
80. Guo X, Huang S, Fu X, Wang B, Huang X. Vascular segmentation in hepatic CT images using adaptive threshold fuzzy connectedness method. Biomed eng online. 2015;14:57.
81. Fabijańska A. Segmentation of pulmonary vascular tree from 3D CT thorax scans. Biocybern Biomed Eng. 2015;35(2):106-19.
82. Chen W, Xu J, Chiu B. Fast segmentation of the femoral arteries from 3D MR images: A tool for rapid assessment of peripheral arterial disease. Med Phys. 2015;42(5):2431-48.
83. Limbu YR, Gurung G Fau - Malla R, Malla R Fau - Rajbhandari R, Rajbhandari R Fau - Regmi SR, Regmi SR. Assessment of carotid artery dimensions by ultrasound in non-smoker healthy adults of both sexes. (2676-1319 (Print)).
84. Qiu Y, Jia Y, Cai H, Li Z, Song C, Feng S. [Changes in diameter of superior mesenteric vein and gastrocolic trunk in patients with cecum-ascending colon cancer]. (1671-0274 (Print)).

85. Zhang Y, Zhang X, Chang R, Cang P, Liu X, Xia Q. Diameter measurements of cerebral arteries on three-dimensional time-of-flight MR angiograms. Chinese Journal of Radiology. 2003;37(5):394-8.
86. Bullitt E ZD, Gerig G, Aylward S, Joshi S, Smith JK, Lin W, Ewend MG. Vessel tortuosity and brain tumor malignancy: A blinded study. Academic Radiology. 2005;12:1232-40.
87. Ramadan SU, Yiğit H Fau - Gökharman D, Gökharman D Fau - Tunçbilek I, Tunçbilek I Fau - Dolgun NA, Dolgun Na Fau - Koşar P, Koşar P Fau - Koşar U, et al. Can renal dimensions and the main renal artery diameter indicate the presence of an accessory renal artery? A 64-slice CT study. (1305-3612 (Electronic)).
88. Gagnon AR BP. Deep and Superficial Inferior Epigastric Artery Perforator Flaps. Cirugía Plástica Ibero-Latinoamericana. 2006;32(4):7-13.
89. Gameraddin M. Normal abdominal aorta diameter on abdominal sonography in healthy asymptomatic adults: impact of age and gender. Journal of Radiation Research and Applied Sciences. 2019;12(1):186-91.
90. Holzer R, Qureshi S Fau - Ghasemi A, Ghasemi A Fau - Vincent J, Vincent J Fau - Sievert H, Sievert H Fau - Gruenstein D, Gruenstein D Fau - Weber H, et al. Stenting of aortic coarctation: acute, intermediate, and long-term results of a prospective multi-institutional registry--Congenital Cardiovascular Interventional Study Consortium (CCISC). (1522-726X (Electronic)).
91. Debbaut C, Segers P, Cornillie P, Casteleyn C, Dierick M, Laleman W, et al. Analyzing the human liver vascular architecture by combining vascular corrosion casting and micro-CT scanning: a feasibility study. J Anat. 2014;224(4):509-17.
92. Soler L HA, Agnus V, Charnoz A, Fasquel J, Moreau J,, Osswald A BM, Marescaux J.) 3D image reconstruction for comparison of algorithm database: A patient specific
anatomical and medical image database. 2010.
93. Townsley MI. Structure and composition of pulmonary arteries, capillaries, and veins. Compr Physiol. 2012;2(1):675-709.
94. Zhou FF, Liu Y, Ge PC, Chen ZH, Ding XQ, Liu JY, et al. Coronary Artery Diameter is Inversely Associated with the Severity of Coronary Lesions in Patients Undergoing Coronary Angiography. Cellular Physiology and Biochemistry. 2017;43(3):1247-57.
95. Venditti C, Casselman R, Murphy M, Adamson SL, Sled J, Smith G. Chronic carbon monoxide inhalation during pregnancy augments uterine artery blood flow and uteroplacental vascular growth in mice. American journal of physiology Regulatory, integrative and comparative physiology. 2013;305.
96. Armato SG, 3rd, McLennan G Fau - Bidaut L, Bidaut L Fau - McNitt-Gray MF, McNitt-Gray Mf Fau - Meyer CR, Meyer Cr Fau - Reeves AP, Reeves Ap Fau - Zhao B, et al. The Lung Image Database Consortium (LIDC) and Image Database Resource Initiative (IDRI): a completed reference database of lung nodules on CT scans. (0094-2405 (Print)).
97. Frangi R, Niessen WJ, Vincken K, Viergever M. Multiscale Vessel Enhancement Filtering. Med Image Comput Comput Assist Interv. 2000;1496.
98. Milnerowicz S, Milnerowicz A, Taboła R. A middle mesenteric artery. Surg Radiol Anat. 2012;34(10):973-5.
99. http://www.ircad.fr/research/3d-ircadb-01/, 149–153. [
100. Heimann T, van Ginneken B Fau - Styner MA, Styner Ma Fau - Arzhaeva Y, Arzhaeva Y Fau - Aurich V, Aurich V Fau - Bauer C, Bauer C Fau - Beck A, et al.

Comparison and evaluation of methods for liver segmentation from CT datasets. (1558-254X (Electronic)).
101. Hamarneh G, Jassi P. VascuSynth: Simulating vascular trees for generating volumetric image data with ground-truth segmentation and tree analysis. Computerized Medical Imaging and Graphics. 2010;34(8):605-16.
102. Arnez ZM, Valdatta L Fau - Tyler MP, Tyler Mp Fau - Planinsek F, Planinsek F. Anatomy of the internal mammary veins and their use in free TRAM flap breast reconstruction. (0007-1226 (Print)).
103. van den Bouwhuijsen QJA, Vernooij MW, Hofman A, Krestin GP, van der Lugt A, Witteman JCM. Determinants of magnetic resonance imaging detected carotid plaque components: the Rotterdam Study. European Heart Journal. 2012;33(2):221-9.
104. Vital hwvc.
105. Spector KS, Lawson WE. Optimizing safe femoral access during cardiac catheterization. Catheterization and Cardiovascular Interventions. 2001;53(2):209-12.
106. Lo P, van Ginneken B, Reinhardt J, Yavarna T, de Jong P, Irving B, et al. Extraction of airways from CT (EXACT'09). IEEE Transactions on Medical Imaging. 2012;31(11):2093-107.
107. Lin E, Alessio A. What are the basic concepts of temporal, contrast, and spatial resolution in cardiac CT? J Cardiovasc Comput Tomogr. 2009;3(6):403-8.

Appendix – Search Strings

Embase.com

('virtual reality'/de OR 'augmented reality'/de OR 'mixed reality'/de OR 'immersive virtual reality'/de OR 'three-dimensional imaging'/de OR (((virtual* OR augment* OR extended OR merged) NEAR/3 (realit* OR environment*)) OR mixed-reality OR virtualreality OR Hologra* OR (immersive NEAR/3 (experience* OR technolog*)) OR ((three-dimensional OR 3-dimensional OR 3d OR 3-d) NEAR/3 (imag* OR visuali*))):ab,ti OR (vr):ti) AND ('artificial intelligence'/de OR 'ambient intelligence'/de OR 'machine learning'/exp OR 'computer vision'/de OR algorithm/de OR (((ambient* OR artificial*) NEAR/3 intelligence) OR ((machine OR deep OR network) NEXT/2 learning) OR learning-based OR ((neural* OR neurol*) NEAR/3 network*) OR (feature* NEAR/3 (detection OR extraction* OR learning OR ranking OR selection)) OR Computer-vision* OR (Computer NEAR/3 (Aided OR assisted) NEAR/3 Detect*) OR algorithm* OR support-vector* OR random-forest* OR fuzzy OR k-nearest* OR back-propagation OR heuristic* OR dimensionality-reduction OR time-warping OR mode-decomposition OR kernel OR closest-point* OR markov OR locality-sensitive-hashing OR maximum-likelihood OR model-predictive-control OR radial-basis-function OR recursive-partitioning):Ab,ti) AND ('computer assisted tomography'/exp OR 'nuclear magnetic resonance imaging'/exp OR ((compute* NEAR/3 tomogra*) OR ((ct OR cat) NEXT/1 scan*) OR (magnetic NEAR/3 resonan*) OR mri OR mr-imag* OR mvct):ab,ti OR (ct OR mr):ti) AND ('blood vessel'/exp OR vascularization/de OR angiography/exp OR 'blood flow'/exp OR (vessel* OR vascul* OR microvessel* OR microvascul* OR (blood NEAR/3 (supply* OR flow)) OR arter* OR angiogra* OR vein* OR venous):ab,ti) NOT ([conference abstract]/lim AND [2000-2018]/py) AND [english]/lim NOT ([animals]/lim NOT [humans]/lim)

Medline ALL Ovid

(Virtual Reality / OR Augmented Reality / OR Imaging, Three-Dimensional / OR (((virtual* OR augment* OR extended OR merged) ADJ3 (realit* OR environment*)) OR mixed-reality OR virtualreality OR Hologra* OR (immersive ADJ3 (experience* OR technolog*)) OR ((three-dimensional OR 3-dimensional OR 3d OR 3-d) ADJ3 (imag* OR visuali*))).ab,ti. OR (vr).ti.) AND (exp Artificial Intelligence / OR exp Ambient Intelligence / OR exp Machine Learning / OR exp Algorithms / OR (((ambient* OR artificial*) ADJ3 intelligence) OR ((machine OR deep OR network) ADJ2 learning) OR learning-based OR ((neural* OR neurol*) ADJ3 network*) OR (feature* ADJ3 (detection OR extraction* OR learning OR ranking OR selection)) OR Computer-vision* OR (Computer ADJ3 (Aided OR assisted) ADJ3 Detect*) OR algorithm* OR support-vector* OR random-forest* OR fuzzy OR k-nearest* OR back-propagation OR heuristic* OR dimensionality-reduction OR time-warping OR mode-decomposition OR kernel OR closest-point* OR markov OR locality-sensitive-hashing OR maximum-likelihood OR model-predictive-control OR radial-basis-function OR recursive-partitioning).ab,ti.) AND (Tomography, X-Ray Computed / OR exp Magnetic Resonance Imaging/ OR ((compute* ADJ3 tomogra*) OR ((ct OR cat) ADJ scan*) OR (magnetic ADJ3 resonan*) OR mri OR mr-imag* OR mvct).ab,ti. OR (ct OR mr).ti.) AND (exp Blood Vessels/ OR exp Angiography/ OR exp Blood Circulation/ OR (vessel* OR vascul* OR microvessel* OR microvascul* OR (blood ADJ3 (supply* OR flow)) OR arter* OR angiogra* OR vein* OR venous).ab,ti.) AND english.la. NOT (exp animals/ NOT humans/)

Web of Science

TS=(((((virtual* OR augment* OR extended OR merged) NEAR/2 (realit* OR environment*)) OR mixed-reality OR virtualreality OR Hologra* OR (immersive NEAR/2 (experience* OR technolog*)) OR ((three-dimensional OR 3-dimensional OR 3d OR 3-d) NEAR/2 (imag* OR visuali*))) OR (vr):ti) AND ((((ambient* OR artificial*) NEAR/2 intelligence) OR ((machine OR deep OR network) NEAR/2 learning) OR learning-based OR ((neural* OR neurol*) NEAR/2 network*) OR (feature* NEAR/2 (detection OR extraction* OR learning OR ranking OR selection)) OR Computer-vision* OR (Computer NEAR/2 (Aided OR assisted) NEAR/2 Detect*) OR algorithm* OR support-vector* OR random-forest* OR fuzzy OR k-nearest* OR back-propagation OR heuristic* OR dimensionality-reduction OR time-warping OR mode-decomposition OR kernel OR closest-point* OR markov OR locality-sensitive-hashing OR maximum-likelihood OR model-predictive-control OR radial-basis-function OR recursive-partitioning)) AND (((compute* NEAR/2 tomogra*) OR ((ct OR cat) NEAR/1 scan*) OR (magnetic NEAR/2 resonan*) OR mri OR mr-imag* OR mvct) OR (ct OR mr):ti) AND ((vessel* OR vascul* OR microvessel* OR microvascul* OR (blood NEAR/2 (supply* OR flow)) OR arter* OR angiogra* OR vein* OR venous)) NOT ((animal* OR murine OR mouse OR mice OR rats OR rat) NOT (human* OR patient*))) AND DT=(article) AND LA=(english)

Cochrane CENTRAL register of Trials

((((virtual* OR augment* OR extended OR merged) NEAR/3 (realit* OR environment*)) OR mixed NEXT reality OR virtualreality OR Hologra* OR (immersive NEAR/3 (experience* OR technolog*)) OR ((three NEXT dimensional OR 3 NEXT dimensional OR 3d OR 3 NEXT d) NEAR/3 (imag* OR visuali*))):ab,ti OR (vr):ti) AND ((((ambient* OR artificial*) NEAR/3 intelligence) OR ((machine OR deep OR network) NEXT/2 learning) OR learning NEXT based OR ((neural* OR neurol*) NEAR/3 network*) OR (feature* NEAR/3 (detection OR extraction* OR learning OR ranking OR selection)) OR Computer NEXT vision* OR (Computer NEAR/3 (Aided OR assisted) NEAR/3 Detect*) OR algorithm* OR support NEXT vector* OR random NEXT forest* OR fuzzy OR k NEXT nearest* OR back NEXT propagation OR heuristic* OR dimensionality NEXT reduction OR time NEXT warping OR mode NEXT decomposition OR kernel OR closest NEXT point* OR markov OR locality NEXT sensitive NEXT hashing OR maximum NEXT likelihood OR model NEXT predictive NEXT control OR radial NEXT basis NEXT function OR recursive NEXT partitioning):Ab,ti) AND (((compute* NEAR/3 tomogra*) OR ((ct OR cat) NEXT/1 scan*) OR (magnetic NEAR/3 resonan*) OR mri OR mr NEXT imag* OR mvct):ab,ti OR (ct OR mr):ti) AND ((vessel* OR vascul* OR microvessel* OR microvascul* OR (blood NEAR/3 (supply* OR flow)) OR arter* OR angiogra* OR vein* OR venous):ab,ti)

Google Scholar

"virtual|augment|extended|merged reality" "artificial intelligence"|"machine|deep learning" "computer*tomography"|"computer tomography"|"ct|cat scan"|"magnetic resonance"|mri vessels|vascular|microvessels|microvasculular|"blood supply|flow"|angiography

B. Questionnaire

Questionnaire Experiments Tessa Kos

This questionnaire consists of an adaptation of the standardized USE questionnaire. After each section, you will have space for adding remarks. Please feel free to put down anything you find remarkable.

Thank you in advance for your participation!

* Vereist

Participant characteristics

1. This questionnaire is anonymous. I agree that these results can be used for research purposes. *

- ◯ I agree
- ◯ I disagree

2. I am *

- ◯ Staff
- ◯ AIOS

3. X years experience with breast reconstructions *

- ◯ 0-5
- ◯ 5-10
- ◯ 10-15
- ◯ >15

4. I agree to be part of the 'expert group', used for gold standard comparison (if yes, please leave your name in the next box) *

- ◯ Yes
- ◯ No

5. Name: *

6. Participated in X breast reconstructions *

- ◯ 0-10
- ◯ 10-20
- ◯ 20-30
- ◯ >30

Conventional CTA

7. The following perforator characteristic was visible for assessment: *

	Strongly disagree			Neutral			Strongly agree
Calibre	◯	◯	◯	◯	◯	◯	◯
Intramuscular course	◯	◯	◯	◯	◯	◯	◯
Location in flap	◯	◯	◯	◯	◯	◯	◯
Perforator origin	◯	◯	◯	◯	◯	◯	◯
Subcutaneous branching	◯	◯	◯	◯	◯	◯	◯
Connection surrounding vessels	◯	◯	◯	◯	◯	◯	◯

8. What is/are your main consideration(s) for selecting this perforator? *

9. Usefulness *

	Strongly disagree			Neutral			Strongly agree
Conventional planning is useful	○	○	○	○	○	○	○
Conventional planning meets my needs	○	○	○	○	○	○	○
Conventional planning meets my expectations	○	○	○	○	○	○	○
Conventional planning saves me operative time	○	○	○	○	○	○	○

10. Ease of Use *

	Strongly disagree			Neutral			Strongly agree
Conventional planning is easy to use	○	○	○	○	○	○	○
Conventional planning is user friendly	○	○	○	○	○	○	○
After initial training, I can use conventional planning without written instructions	○	○	○	○	○	○	○
Conventional planning requires the fewest steps possible to accomplish what I want to do with it	○	○	○	○	○	○	○
After initial training, using conventional planning is effortless	○	○	○	○	○	○	○
With conventional planning, I can recover from mistakes quickly and easily	○	○	○	○	○	○	○

11. Ease of learning *

	Strongly disagree			Neutral			Strongly agree
It is easy to learn to use conventional planning	○	○	○	○	○	○	○
I quickly became skillful with conventional planning	○	○	○	○	○	○	○

12. Satisfaction *

	Strongly disagree			Neutral			Strongly agree
I am satisfied with conventional planning	○	○	○	○	○	○	○
I would recommend conventional planning to a collegue	○	○	○	○	○	○	○
I feel I need to have conventional planning	○	○	○	○	○	○	○
Conventional planning is fun to use	○	○	○	○	○	○	○

The 3D model

13. The following perforator characteristic was visible for assessment: *

	Strongly disagree			Neutral			Strongly agree
Calibre	○	○	○	○	○	○	○
Intramuscular course	○	○	○	○	○	○	○
Location in flap	○	○	○	○	○	○	○
Perforator origin	○	○	○	○	○	○	○
Subcutaneous branching	○	○	○	○	○	○	○
Connection surrounding vessels	○	○	○	○	○	○	○

14. What is/are your main consideration(s) for selecting this perforator? *

15. Usefulness *

	Strongly disagree			Neutral			Strongly agree
The 3D model is useful	○	○	○	○	○	○	○
The 3D model meets my needs	○	○	○	○	○	○	○
The 3D model meets my expectations	○	○	○	○	○	○	○
The 3D model saves me time compared to conventional planning	○	○	○	○	○	○	○

16. Ease of Use *

	Strongly disagree			Neutral			Strongly agree
The 3D model is easy to use	○	○	○	○	○	○	○
The 3D model is user friendly	○	○	○	○	○	○	○
After initial training, I can use the 3D model without written instructions	○	○	○	○	○	○	○
The 3D model requires the fewest steps possible to accomplish what I want to do with it	○	○	○	○	○	○	○
After initial training, using the 3D model is effortless	○	○	○	○	○	○	○
With the 3D model, I can recover from mistakes quickly and easily	○	○	○	○	○	○	○

17. Ease of learning *

	Strongly disagree			Neutral			Strongly agree
It is easy to learn to use the 3D model	○	○	○	○	○	○	○
I quickly became skillful with the 3D model	○	○	○	○	○	○	○

18. Satisfaction *

	Strongly disagree			Neutral			Strongly agree
I am satisfied with the 3D model	○	○	○	○	○	○	○
I would recommend using the 3D model to a collegue	○	○	○	○	○	○	○
The 3D model works the way I want it to work	○	○	○	○	○	○	○
I feel I need to have the 3D model	○	○	○	○	○	○	○
The 3D model is fun to use	○	○	○	○	○	○	○

19. I prefer to use the 3D model with a visible CTA *

- ○ Yes
- ○ No

20. I prefer to use the 3D model with a cutting plane *

- ○ Yes
- ○ No

21. A 3D model would improve preoperative planning of DIEP flaps *

- ◯ Yes
- ◯ No

22. I would prefer: *

- ◯ A 3D model **instead of** conventional planning
- ◯ A 3D model **in addition to** conventional planning
- ◯ No 3D model

The VR model

23. The following perforator characteristic was visible for assessment: *

	Strongly disagree			Neutral			Strongly agree
Calibre	◯	◯	◯	◯	◯	◯	◯
Intramuscular course	◯	◯	◯	◯	◯	◯	◯
Location in flap	◯	◯	◯	◯	◯	◯	◯
Perforator origin	◯	◯	◯	◯	◯	◯	◯
Subcutaneous branching	◯	◯	◯	◯	◯	◯	◯
Connection surrounding vessels	◯	◯	◯	◯	◯	◯	◯

24. What is/are your main consideration(s) for selecting this perforator? *

25. Usefulness *

	Strongly disagree			Neutral			Strongly agree
The VR model is useful	○	○	○	○	○	○	○
The VR model meets my needs	○	○	○	○	○	○	○
The VR model meets my expectations	○	○	○	○	○	○	○
The VR model saves me time compared to conventional planning	○	○	○	○	○	○	○

26. Ease of Use *

	Strongly disagree			Neutral			Strongly agree
The VR model is easy to use	○	○	○	○	○	○	○
The VR model is user friendly	○	○	○	○	○	○	○
After initial training, I can use the VR model without written instructions	○	○	○	○	○	○	○
The VR model requires the fewest steps possible to accomplish what I want to do with it	○	○	○	○	○	○	○
After initial training, using the VR model is effortless	○	○	○	○	○	○	○
With the VR model, I can recover from mistakes quickly and easily	○	○	○	○	○	○	○

27. Ease of learning *

	Strongly disagree			Neutral			Strongly agree
It is easy to learn to use the VR model	○	○	○	○	○	○	○
I quickly became skillful with the VR model	○	○	○	○	○	○	○

28. Satisfaction *

	Strongly disagree			Neutral			Strongly agree
I am satisfied with the VR model	○	○	○	○	○	○	○
I would recommend using the VR model to a collegue	○	○	○	○	○	○	○
The VR model works the way I want it to work	○	○	○	○	○	○	○
I feel I need to have the VR model	○	○	○	○	○	○	○
The VR model is fun to use	○	○	○	○	○	○	○

29. A VR model would improve preoperative planning of DIEP flaps *

- ○ Yes
- ○ No

30. I would prefer: *

- ○ The VR model **instead of** conventional planning
- ○ The VR model **in addition to** conventional planning
- ○ No VR model

Overall opinion

31. I prefer: *

- ◯ Conventional planning
- ◯ 3D model
- ◯ VR model

32. Closing remarks:

C. Questionnaire results

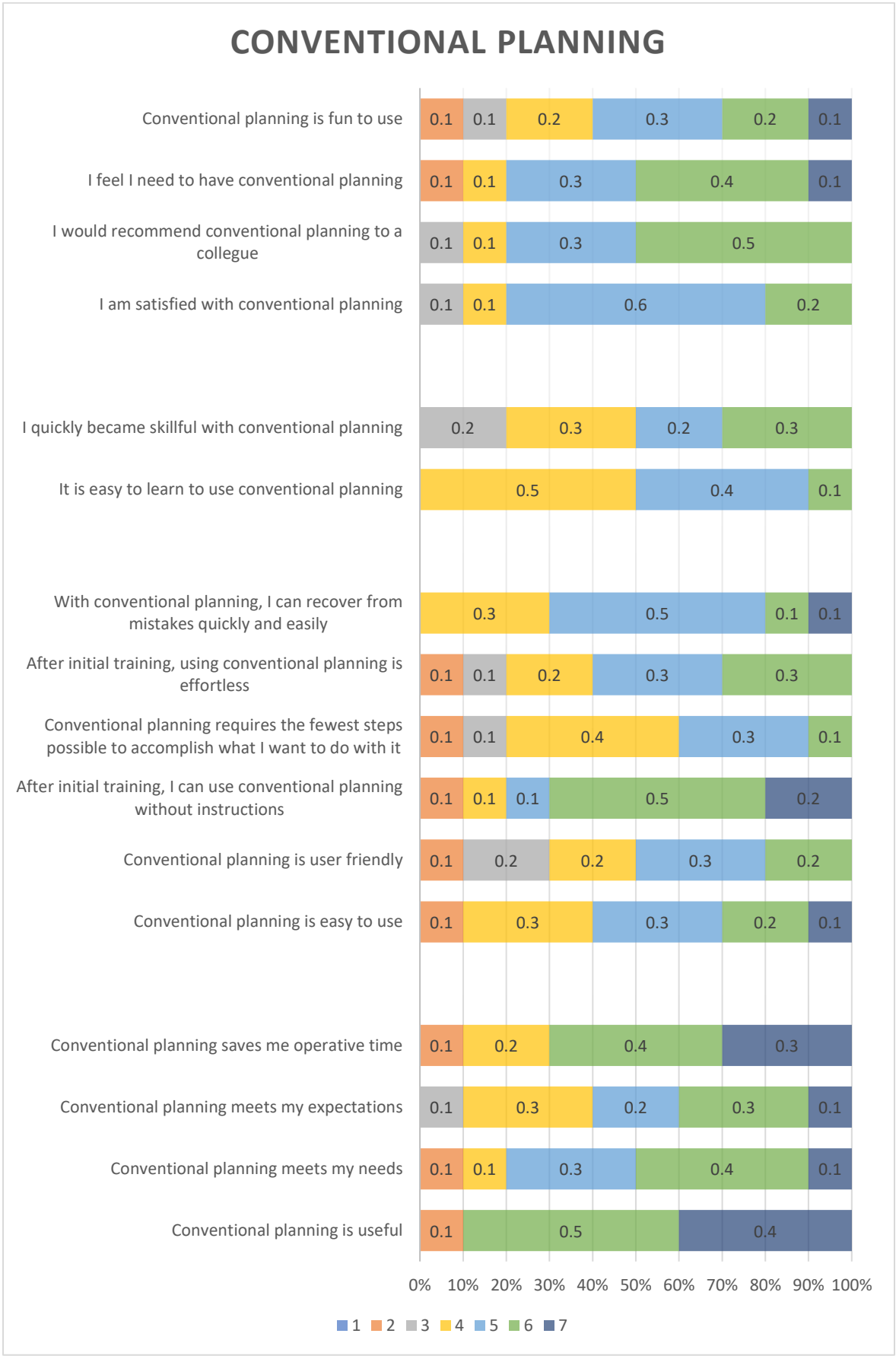

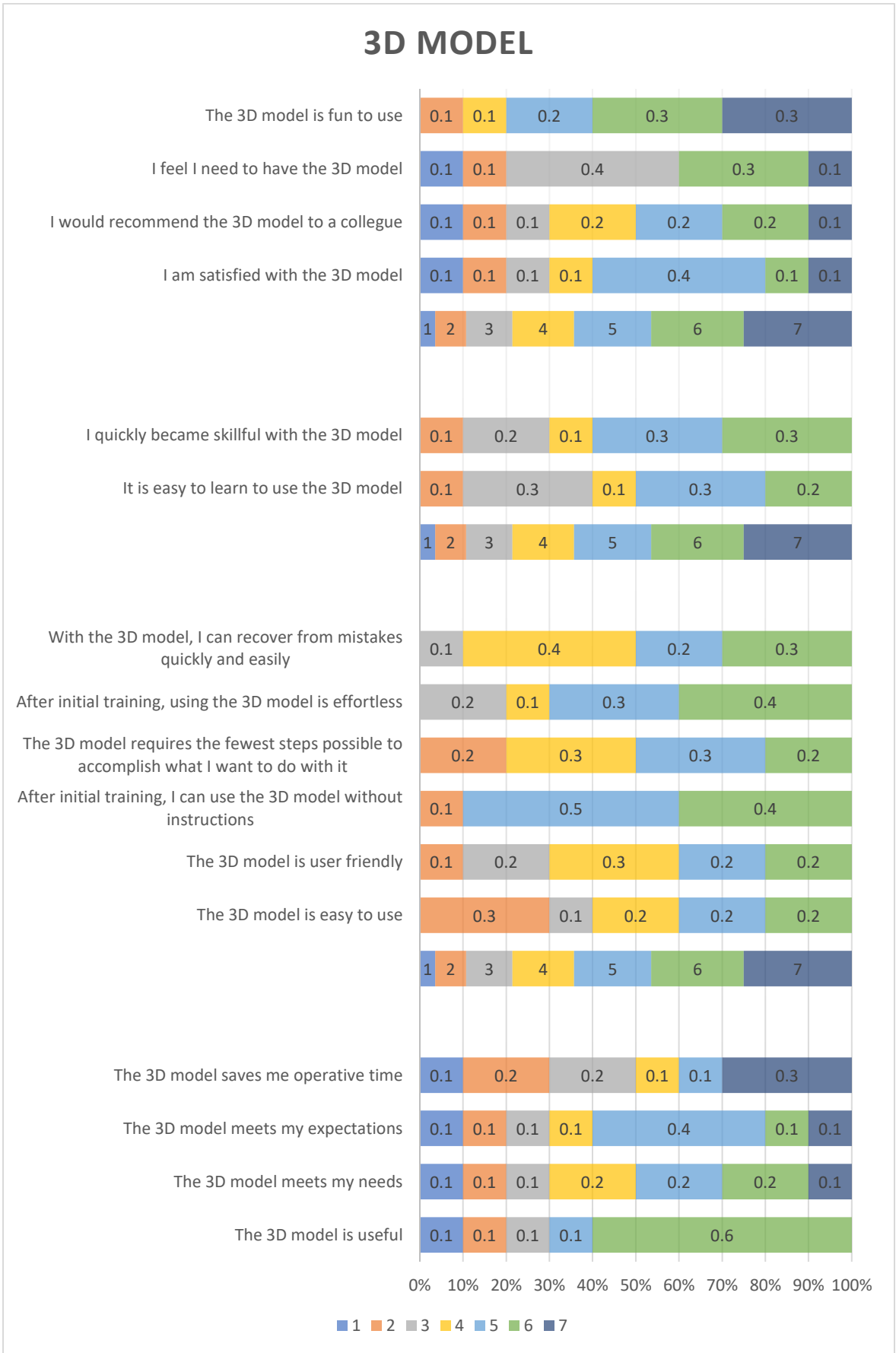
3D MODEL
The 3D model is fun to use
0.1 0.1 0.2 0.3 0.3
I feel I need to have the 3D model
0.1 0.1 0.4 0.3 0.1
I would recommend the 3D model to a collegue
0.1 0.1 0.1 0.2 0.2 0.2 0.1
I am satisfied with the 3D model
0.1 0.1 0.1 0.1 0.4 0.1 0.1
1 2 3 4 5 6 7
I quickly became skillful with the 3D model
0.1 0.2 0.1 0.3 0.3
It is easy to learn to use the 3D model
0.1 0.3 0.1 0.3 0.2
1 2 3 4 5 6 7
With the 3D model, I can recover from mistakes quickly and easily
0.1 0.4 0.2 0.3
After initial training, using the 3D model is effortless
0.2 0.1 0.3 0.4
The 3D model requires the fewest steps possible to accomplish what I want to do with it
0.2 0.3 0.3 0.2
After initial training, I can use the 3D model without instructions
0.1 0.5 0.4
The 3D model is user friendly
0.1 0.2 0.3 0.2 0.2
The 3D model is easy to use
0.3 0.1 0.2 0.2 0.2
1 2 3 4 5 6 7
The 3D model saves me operative time
0.1 0.2 0.2 0.1 0.1 0.3
The 3D model meets my expectations
0.1 0.1 0.1 0.1 0.4 0.1 0.1
The 3D model meets my needs
0.1 0.1 0.1 0.2 0.2 0.2 0.1
The 3D model is useful
0.1 0.1 0.1 0.1 0.6
0% 10% 20% 30% 40% 50% 60% 70% 80% 90% 100%
1 2 3 4 5 6 7

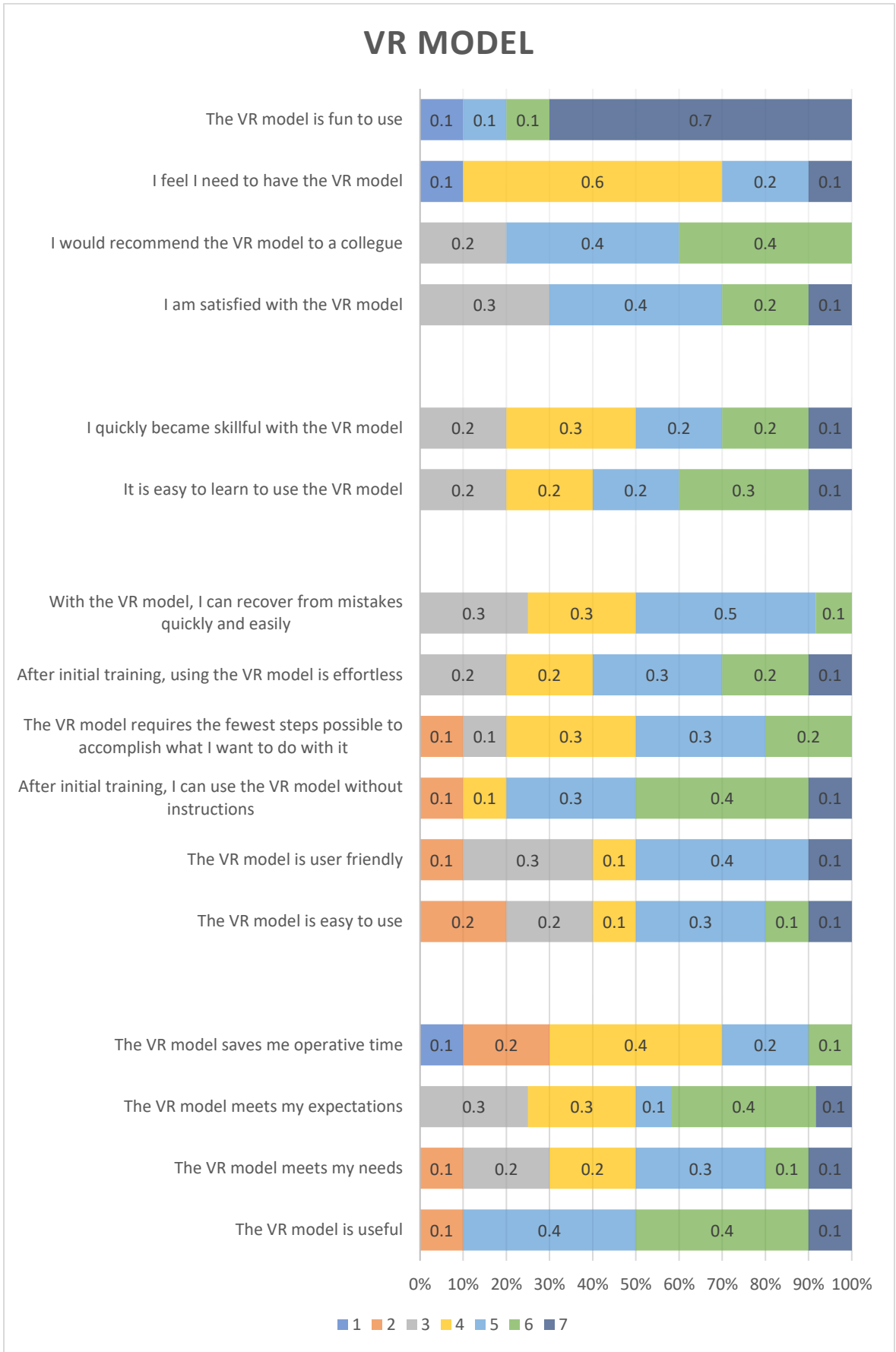
VR MODEL
The VR model is fun to use
0.1 0.1 0.1 0.7
I feel I need to have the VR model
0.1 0.6 0.2 0.1
I would recommend the VR model to a collegue
0.2 0.4 0.4
I am satisfied with the VR model
0.3 0.4 0.2 0.1
I quickly became skillful with the VR model
0.2 0.3 0.2 0.2 0.1
It is easy to learn to use the VR model
0.2 0.2 0.2 0.3 0.1
With the VR model, I can recover from mistakes quickly and easily
0.3 0.3 0.5 0.1
After initial training, using the VR model is effortless
0.2 0.2 0.3 0.2 0.1
The VR model requires the fewest steps possible to accomplish what I want to do with it
0.1 0.1 0.3 0.3 0.2
After initial training, I can use the VR model without instructions
0.1 0.1 0.3 0.4 0.1
The VR model is user friendly
0.1 0.3 0.1 0.4 0.1
The VR model is easy to use
0.2 0.2 0.1 0.3 0.1 0.1
The VR model saves me operative time
0.1 0.2 0.4 0.2 0.1
The VR model meets my expectations
0.3 0.3 0.1 0.4 0.1
The VR model meets my needs
0.1 0.2 0.2 0.3 0.1 0.1
The VR model is useful
0.1 0.4 0.4 0.1
0% 10% 20% 30% 40% 50% 60% 70% 80% 90% 100%
1 2 3 4 5 6 7

D. Additional comments questionnaire (literal transcription)

Subject ID	Remarks
1	Het 3D model was voor mij weinig meerwaarde omdat je de locatie in de lap er niet makkelijk bij ziet, dus het ook lastig is de beste te kiezen. De vragen of het model makkelijk te leren is en zonder schriftelijke instructies te gebruiken zijn niet te beantwoorden na 1 keer gebruiken met continue hulp. Het VR model geeft de vaten prachtig weer en je ziet goed waar die in de lap zitten, maar ik vond het lastig te zien welk deel precies intramusculair loopt en ik heb geen metingen genomen die ik op de patient zou kunnen zetten. Ook hier kan ik niet beoordelen of het makkelijk aan te leren is. Sommige dingen, zoals kaliber van de vaten, zijn goed beoordeelbaar, maar ik weet niet of dat ook matcht met de conventionele CT en of het matcht met de vaten in de patient... dus zonder correlatie met de CT (het enige wat ik ken en wat ik nu dus ook nog echt ernaast nodig zou hebben om 'veilig' te werken) en echte situatie. In de begin fase zal het denk ik beschikbaar moeten zijn naast de conventionele CT, om als operateur zelf het gevoel te krijgen hoe goed het beeld matcht en of de conventionele daardoor weg gelaten kan worden. Ik was niet sneller met de VR planning dan met beoordeling conventionele CT.
2	I feel the segmentation leads to overestimation of the caliber of the smaller vessels/perforators.
3	Betere vergelijking kaliber perforatoren. Beloop en origin beter met VR. DUs met conventioneel alleen kom je er ook. VR een goede aanvulling.
4	Als ik morgen een DIEP zou moeten doen ben ik nog te weinig getraind om mijn planning volledig op 3d en VR te doen, ook omdat ik de markeringen wil overbrengen op de buik vd patient en toch daarvoor metingen moet doen nog. Als ik beter bekwaam zou zijn zou ik denk ik selectie willen doen op VR of 3D en metingen dan nameten op conventioneel / als export willen hebben van mijn markering
5	bij selectie perforator coordinaten kunnen vastleggen (of ar). de perforator volgen als een vliegtuig door de spier heen. mot zenuwen visualiseren?
6	I think the 3D model is the easiest option and it is good enough for me.
7	More use of 3d and VR needed. I chose conventional b/c I am used to that and I am quicker with that.
8	nog ver van mijn bed show. VR supermooi maar ik moet nog wennen denk ik. 3D met conventionele CT-scan is ook top
9	subcutaneuos branching in all 3 types of plannng not very cear
10	Bij VR zie je duidelijker het subcutane beloop van de vaten, maar ik denk niet dat het essentieel is om toe te voegen aan conventionele CT of 3D.